

Inference post Selection of Group-sparse Regression Models

Snigdha Panigrahi

Department of Statistics, University of Michigan

and

Peter W. MacDonald

Department of Statistics, University of Michigan

and

Daniel Kessler

Departments of Statistics and Psychiatry, University of Michigan

Abstract

Conditional inference provides a rigorous approach to counter bias when data from automated model selections is reused for inference. We develop in this paper a statistically consistent Bayesian framework to assess uncertainties within linear models that are informed by grouped sparsities in covariates. Finding wide applications when genes, proteins, genetic variants, neuroimaging measurements are grouped respectively by their biological pathways, molecular functions, regulatory regions, cognitive roles, these models are selected through a useful class of group-sparse learning algorithms. An adjustment factor to account precisely for the selection of promising groups, deployed with a generalized version of Laplace-type approximations is the centerpiece of our new methods. Accommodating well known group-sparse models such as those selected by the Group LASSO, the overlapping Group LASSO, the sparse Group LASSO etc., we illustrate the efficacy of our methodology in extensive experiments and on data from a human neuroimaging application.

1 Introduction

Learning models with meaning and assessing uncertainties for the matched parameters are an integral part of analyzing large structured datasets. Without appropriate adjustments for the bias from automated model selections, inference reusing the same data lacks statistical validity of any kind [Benjamini and Yekutieli, 2005, Berk et al., 2013, Kuffner and Young, 2017, Guo and He, 2020]. A conditional inferential approach, developed in Lee et al. [2016], Tibshirani et al. [2016] among others, reinstates inferential reliability by enabling a reuse of data from the selection steps. Assuming prominence when principled learning algorithms guide uncertainty estimation, conditioning is motivated by an allocation of residual information from selection towards inferential tasks.

Our paper develops novel conditional techniques to ascertain uncertainties in linear models informed by grouped sparsities in covariates. Working within a regression setting, the key assumptions for our problem are as follows: (i) the covariates act naturally in groups known a priori in the analysis; (ii) only a few of these groups of variables affect the outcome, captured effectively by a parsimonious model. Models ignoring these grouped sparsity structures entirely, such as those selected by the LASSO [Tibshirani, 1996], might fail to characterize outcome variability with accuracy. Significant progress evidently has been made to develop an indispensable class of learning algorithms that select relevant models exploiting this knowledge about the covariate space [Yuan and Lin, 2005, Jacob et al., 2009a, Obozinski et al., 2011, Simon et al., 2013]. The resulting group-sparse models find uses in diverse applications, for example, linking genes grouped by pathways to clinical outcomes [Park et al., 2015, Xie et al., 2019], using brain imaging features grouped by anatomical area or network properties to predict psychiatric diagnosis or to decode stimulus type [Relión et al., 2019, Shimizu et al., 2015, Rao et al., 2016].

Conditional tools truncating realizations to a selection event rely upon an analytic description of the same event. This description admits an affine form for the well-studied

LASSO, which means that the selection event is expressed as linear inequalities in terms of the involved data variables [Lee et al., 2016, Tian and Taylor, 2018]. Characterizing explicitly the selection of groups, let alone an affine representation poses the foremost difficulty in subsequent inference [Yang et al., 2016, see Section 3.4]. To this end, a posterior we construct after the selection of promising groups and the techniques we develop thereafter to tackle with a complicated (non-affine) geometry associated with this event steer our methodological advances.

Reusing data for efficient uncertainty estimation within group-sparse models, we provide our main contributions below. One, our appealingly resolvable methods pay only a nominal price to correct for the selection-informed nature of our models in comparisons to naive inference, demonstrated extensively in our experiments. Particularly noteworthy, the framework we adopt is easily amenable to data carving [Fithian et al., 2014, Panigrahi, 2018] wherein selection operates only on a subset of the samples. Yet we resourcefully borrow the residual information from the first stage to reuse these samples for considerably more powerful inference. Two, the Bayesian approach we take by sampling from a posterior after selection readily yields us inference for a very flexible set of context-relevant targets, including group-wise maximal magnitudes, sizes etc.. This contrasts sharply with tools that deal with projections of the mean vector for the response onto specific selected subspaces [Loftus and Taylor, 2015, Yang et al., 2016, Rügamer and Greven, 2020]. Three, our proposal encompasses a fairly general class of important group-sparse models targeting different grouped structures. For example, our methods allow selection-informed inference after solving the standardized Group LASSO [Simon and Tibshirani, 2012], overlapping Group LASSO [Jacob et al., 2009a], sparse Group LASSO [Simon et al., 2013].

We present the remaining paper in the following order. Section 2 presents a selection-informed posterior with an adjustment factor to account for the bias from the selection of group-sparse models. In Section 3, we obtain a theoretical value for this highly nontrivial

adjustment factor in our selection-informed posterior. Using a surrogate version of our posterior through a generalized version of Laplace-type approximations yields methods amenable for uncertainty estimation. Next in Section 4, we highlight the generality of our methods in accommodating group-sparse models informed by different forms of grouped structures. Section 5 establishes large-sample theory for our Bayesian methods proving desired concentration properties of our posterior around the underlying parameters. We demonstrate the effectiveness of our inferential methods in numerical experiments and a human neuroimaging application in Section 6. Proofs for our technical results are included in the Supplementary material.

2 Framework for selection-informed inference

We begin by introducing a selection-informed posterior for a group-sparse linear model after selection. Reviewing the affine nature of selections encountered with an ℓ_1 -penalty, we bring to the fore a breakdown of this geometry with a Group LASSO penalty [Yuan and Lin, 2005]. The bottleneck we recognize here leads to our advances in the next section.

2.1 Basic setup

Establishing notations, we observe independent instances of a scalar response variable Y_i and a p -dimensional vector of covariates X_i for $i = 1, \dots, n$. We denote the entire response vector by $y = (Y_1, \dots, Y_n)^\top \in \mathbb{R}^n$ and the corresponding predictor matrix by $\mathbf{X} = (X_1, \dots, X_n)^\top \in \mathbb{R}^{n \times p}$. Throughout this paper we will work in a fixed \mathbf{X} regression setting. Consistent with a selective inferential paradigm, our problem proceeds in two stages: first, we select promising groups by optimizing a learning objective inducing grouped sparsities; then, we specify a group-sparse linear model relying upon the structure we learn from the previous stage.

Our primary case study for exposition will be non-overlapping groupings defined by a

prespecified partition, \mathcal{G} , of our p covariates into G groups. In general, we refer to a group in \mathcal{G} by lowercase g , and $|g| \in \mathbb{N}$ will denote the number of predictors within group g . As we will see later, this structure we assume is simply a prototype in a larger category of grouped sparsities that our methods successfully encompass. We focus for now on the familiar Group LASSO objective [Yuan and Lin, 2005] with added randomization:

$$\hat{\beta}^{(\mathcal{G})} \in \underset{\beta}{\operatorname{argmin}} \left\{ \frac{1}{2} \|y - \mathbf{X}\beta\|_2^2 + \sum_{g \in \mathcal{G}} \lambda_g \|\beta_g\|_2 - \omega^\top \beta \right\}, \quad (1)$$

to select a model aware of these grouped sparsities. Note, for each group $g \in \mathcal{G}$, $\beta_g \in \mathbb{R}^{|g|}$ is a vector with entries corresponding to predictors in group g , and λ_g is a tuning parameter for this group. In the final term of this objective, $\omega \sim \mathcal{N}_p(0, \Omega)$ is an independent Gaussian randomization variable, proposed in Panigrahi et al. [2019], Panigrahi and Taylor [2019], Panigrahi et al. [2020] for an optimal utility of information within our data towards both selection and inference.

Solving (1) will in particular return a subset of the predictors

$$\hat{E} = \operatorname{supp}(\hat{\beta}^{(\mathcal{G})}), \quad (2)$$

where the support of the randomized Group LASSO estimator respects the prespecified grouping. That is, the selected set of covariates can be written as a union of selected groups in \mathcal{G} , which we represent by $\mathcal{G}_{\hat{E}}$. Finally, letting E be the realized value of \hat{E} , we model our response using a selected model:

$$y \sim \mathcal{N}_n(\mathbf{X}_E \beta_E, \sigma^2 I_n), \quad (3)$$

Completing our model specification, we pose a prior for our parameter:

$$\beta_E \sim \pi, \quad (4)$$

adopting a Bayesian framework for selective inference [Yekutieli, 2012, Panigrahi et al., 2016, Panigrahi and Taylor, 2018]. Next we define our main workforce, a selection-informed posterior using (3) and (4). Two comments are in order here, summarized by the next remark.

Remark 2.1. *First, we assume that the variance parameter σ is known for now. But, following the lines of [Panigrahi et al. \[2016\]](#), the Bayesian approach we take easily deals with the case of unknown variance by treating it as a parameter. Second, the model (3) in principle can be more general, parameterized by a realization, \widehat{E}' , obtained by a deterministic yet arbitrary function of \widehat{E} . We proceed with (3) to simplify the development for our readers, noting that the above flexibilities in modeling indeed fit into our framework.*

2.2 Selection-informed posterior

Before proceeding any further, we define the refitted least squares estimate based on (\mathbf{X}_E, y) :

$$\widehat{\beta}_E = (\mathbf{X}_E^\top \mathbf{X}_E)^{-1} \mathbf{X}_E^\top y,$$

where we assume \mathbf{X}_E is full rank. The selection event of observing a set of covariates E is however a function of not just $\widehat{\beta}_E$ and ω , but also involves the orthogonal projection $N_E = X^\top (I_n - \mathbf{X}_E (\mathbf{X}_E^\top \mathbf{X}_E)^{-1} \mathbf{X}_E^\top) y$, ancillary in our selection-informed model (3).

Letting $\Sigma_E = \sigma^2 (\mathbf{X}_E^\top \mathbf{X}_E)^{-1}$, we use the notation $L(\beta_E; \widehat{\beta}_E, N_E, \omega)$ to represent the naive joint likelihood

$$L(\beta_E; \widehat{\beta}_E, N_E, \omega) = L(\beta_E; \widehat{\beta}_E) \cdot L(N_E) \cdot L(\omega \mid \widehat{\beta}_E, N_E), \quad (5)$$

where $L(N_E)$ and

$$L(\beta_E; \widehat{\beta}_E) \propto \exp \left\{ -\frac{1}{2} (\beta_E - \widehat{\beta}_E)^\top \Sigma_E^{-1} (\beta_E - \widehat{\beta}_E) \right\};$$

represent the marginal likelihood of N_E and $\widehat{\beta}_E$ respectively. The factorization in (5) follows from the independence between $\widehat{\beta}_E$ and N_E . With a Gaussian randomization variable that is independent of our response, we further note

$$L(\omega \mid \widehat{\beta}_E, N_E) = L(\omega) \propto \exp \left\{ -\frac{1}{2} \omega^\top \Omega^{-1} \omega \right\}.$$

The naive (uncorrected) likelihood, $L(\beta_E; \widehat{\beta}_E)$, above clearly does not account for the selection-informed nature of our model (3). Instead, in the conditional inferential spirit, the likelihood we work with is constructed by conditioning upon an event of the form

$$\mathcal{A}_E \subseteq \{(\hat{\beta}_E, N_E, \omega) : \hat{E} = E\}.$$

The conditioning event \mathcal{A}_E (as we will see in our next sections) typically turns out to be a proper subset of the event where we observe the active covariates. Equivalently, this amounts to conditioning on some more information than the selected set of variables. The choice of \mathcal{A}_E is often strategic, done to simplify the geometry of the associated selection region significantly; we make this explicit in our methodological development.

Now we state a selection-informed likelihood, the first component of our posterior. A conditional counterpart for (5) is derived by truncating the joint distribution of these statistics to realizations that lead to observing \mathcal{A}_E and is proportional to

$$L(\beta_E; \hat{\beta}_E) \cdot L(N_E) \cdot L(\omega \mid \hat{\beta}_E, N_E) \cdot \mathbf{1}_{\mathcal{A}_E}(\hat{\beta}_E, N_E, \omega).$$

Our final working version of a selection-informed likelihood is obtained by conditioning further upon the ancillary statistic, N_E and integrating out ω . This gives us the function $L_S(\beta_E; \hat{\beta}_E \mid N_E)$, where we adopt the subscript S to underscore that the likelihood is in fact informed by the selection event. Up to proportionality in β_E , we conclude that $L_S(\cdot; \hat{\beta}_E \mid N_E)$ equals

$$(\mathbb{P}(\mathcal{A}_{E;N_E} \mid \beta_E))^{-1} \cdot L(\beta_E; \hat{\beta}_E) \cdot \int L(\omega \mid \hat{\beta}_E, N_E) \cdot \mathbf{1}_{\mathcal{A}_{E;N_E}}(\hat{\beta}_E, \omega) d\omega, \quad (6)$$

$\mathcal{A}_{E;N_E}$ is the set of $\hat{\beta}_E, \omega$ that result in the event \mathcal{A}_E for the fixed instance N_E and

$$\mathbb{P}(\mathcal{A}_{E;N_E} \mid \beta_E) = \int L(\beta_E; \hat{\beta}_E) \cdot L(\omega \mid \hat{\beta}_E, N_E) \cdot \mathbf{1}_{\mathcal{A}_{E;N_E}}(\hat{\beta}_E, \omega) d\omega d\hat{\beta}_E.$$

Using (6) in conjunction with our prior (4) ultimately yields us our selection-informed posterior distribution for β_E :

$$\log \pi_S(\beta_E \mid \hat{\beta}_E, N_E) \propto \log \pi(\beta_E) + \log L(\beta_E; \hat{\beta}_E) - \log \mathbb{P}(\mathcal{A}_{E;N_E} \mid \beta_E). \quad (7)$$

Notice, we use the subscript S to consistently represent a posterior after selection of promising groups. Evaluating the final term $\mathbb{P}(\mathcal{A}_{E;N_E} \mid \beta_E)$, called the *adjustment factor* in

Panigrahi et al. [2016], is rightly recognized as the prime technical hurdle. Tackling this factor feasibly when the Group LASSO objective is employed to learn a model nonetheless demands novel strategies. This is attributed to the very distinct geometry induced by penalties targeting grouped sparsities, no longer resulting in an immediate affine description for the event associated with the selection of groups, \mathcal{G}_E .

2.3 Breakdown of affine geometry

Emphasized in Section 1, prior methods [Panigrahi and Taylor, 2018, Tian and Taylor, 2018] deal with selection rules that admit an affine (or, asymptotically affine) characterization for the underlying event. A leading example is the randomized LASSO with an ℓ_1 penalty. To be precise, the event \mathcal{A}_E is expressed as linear inequalities in terms of the involved statistics:

$$\mathcal{A}_E = \left\{ (\hat{\beta}_E, N_E, \omega) : \mathbf{A}_E \left((\hat{\beta}_E)^\top \quad (N_E)^\top \right)^\top + \mathbf{B}_E \omega < b_E \right\}, \quad (8)$$

which is why the associated selection is alternately dubbed a Polyhedral event.

To better appreciate this affine geometry we see for the LASSO, suppose that $n = p$, $X = I_n$ and $\lambda = 1$. Then, a randomized version of the LASSO solves

$$\hat{\beta}^{(L)} = \underset{\beta}{\operatorname{argmin}} \frac{1}{2} \|y - \beta\|_2^2 + \|\beta\|_1 - \omega^\top \beta;$$

$\omega \sim N(0, I_n)$. Let E denote the selected set of variables, $-E$ the excluded indices and s the vector of signs for these selected variables. The stationary mapping is summarized by:

$$\begin{pmatrix} \omega_E \\ \omega_{-E} \end{pmatrix} = - \begin{pmatrix} \hat{\beta}_E \\ N_E \end{pmatrix} + \begin{pmatrix} \hat{\beta}_E^{(L)} \\ 0 \end{pmatrix} + \begin{pmatrix} s \\ z \end{pmatrix}, \quad \frac{\partial}{\partial b} (\|\beta\|_1) \Big|_{\hat{\beta}_{\text{LASSO}}} = \begin{pmatrix} s \\ z \end{pmatrix};$$

$\hat{\beta}_E = y_E$ and $N_E = y_{-E}$ (ignoring the coordinates that equal 0). The conditioning event \mathcal{A}_E identified in this instance equals

$$\left\{ \hat{E} = E, \operatorname{sign}(\hat{\beta}_E^{(L)}) = s \right\},$$

including additionally the signs of the nonzero indices of the LASSO solution [Lee et al., 2016].

Note, the event that the LASSO shrinks all the coefficients included in $-E$ to 0 is equivalent to:

$$\|z\|_\infty < 1_{n-|E|} \equiv \|\omega_{-E} + N_E\|_\infty < 1_{n-|E|},$$

resulting in $2(n - |E|)$ linear inequalities. From here, observe that the selecting indices E with the signs s is obtained by further intersecting this region with $|E|$ linear constraints:

$$\text{diag}(s)(\omega_E + \hat{\beta}_E) > 0_{|E|},$$

thereby assuming the affine form in (8).

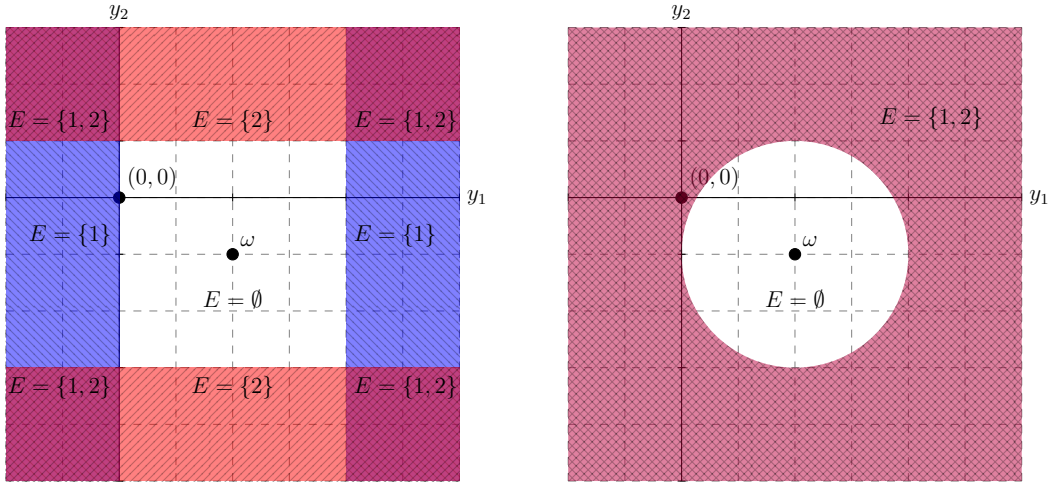


Figure 1: Selection regions for the randomized LASSO (left) and randomized Group LASSO (right) as a function of the observations (y_1, y_2) when the randomization $\omega = (1, -\frac{1}{2})$. The LASSO can select any of $\emptyset, \{1\}, \{2\}$, or $\{1, 2\}$ as predictors by setting the associated entries of $\hat{\beta}$ nonzero. The Group LASSO, on the other hand, can select only \emptyset or $\{1, 2\}$.

The Group LASSO penalty (1) on the other hand exhibits sharply disparate geometry when we set out to analyze the event $\{\hat{E} = E\}$. Continuing with the same instance, the

optimization problem in (1) is now associated with the stationary mapping:

$$\begin{pmatrix} \omega_E \\ \omega_{-E} \end{pmatrix} = - \begin{pmatrix} \hat{\beta}_E \\ N_E \end{pmatrix} + \begin{pmatrix} \hat{\beta}_E^{(\mathcal{G})} \\ 0 \end{pmatrix} + \begin{pmatrix} (\hat{\beta}_g / \|\hat{\beta}_g\|_2)_{g \in \mathcal{G}_E} \\ (z_g)_{g \in -\mathcal{G}_E} \end{pmatrix}, \quad (9)$$

where the final term is the subgradient of the Group LASSO penalty evaluated at the solution. For each non-selected group $g \in -\mathcal{G}_E$, z_g is a vector in $\mathbb{R}^{|g|}$ satisfying $\|z_g\|_2 < 1$, which cannot be expressed in terms of linear inequalities in our variables.

In Figure 1, we provide a pictorial illustration of the discussion above, when $n = p = 2$ for both the LASSO and the Group LASSO in which case the two predictors under consideration comprise a single group. We can then visualize in this plot the selection events as a function of (y_1, y_2) for some fixed $\omega = (\omega_1, \omega_2)$, readily understanding an affine geometry for the Lasso selection event and noting the disparity in the two geometries. Nevertheless, the techniques in this paper allow an explicit analysis of this non-affine selection event for group-sparse models, while providing theoretical guarantees similar in spirit to Panigrahi et al. [2016].

3 Selection-informed inference: our methods

We first identify a theoretical expression for the adjustment factor in our selection-informed posterior (7). With a slight abuse, we will hereafter denote the event $\mathcal{A}_{E;N_E}$ by \mathcal{A}_E to maintain simple notations. That is, our adjustment factor will be represented as $\mathbb{P}(\mathcal{A}_E \mid \beta_E)$. Then we offer methods targeting a statistically consistent surrogate for this posterior and enabling us a framework amenable to (gradient-based) MCMC samplers in general.

We describe below our approach for selection-informed inference after a randomized Group LASSO, deferring to Section 4 the generality of our results in dealing with other grouped sparsities.

3.1 Adjustment factor

We take a first step in our technical progression by obtaining an expression for the adjustment factor, $\mathbb{P}(\mathcal{A}_E \mid \beta_E)$. Along this goal, we recognize a conditioning event \mathcal{A}_E expressed in terms of support constraints on the sizes (Euclidean norms) of our selected groups. We encounter however a nontrivial function in decoding this adjustment factor. We will note that this function dissolves as a constant for the usual LASSO [Panigrahi and Taylor, 2019], and hence does not play a role in selection-informed inference in this more familiar scenario.

To simplify the form of $\mathbb{P}(\mathcal{A}_E \mid \beta_E)$ in (7), we rely on a change of variables by inverting the stationary mapping of the Group LASSO optimization [Tian et al., 2016]. Back to our primary case study of the Group LASSO, we write the non-zero solution for a selected group, g , in polar coordinates:

$$\widehat{\beta}_g^{(\mathcal{G})} = \gamma_g u_g$$

such that $\gamma_g > 0$ represents the size of the selected group and $\|u_g\|_2 = 1$. The stationary mapping associated with (1) is given by:

$$\omega = X^\top X \begin{pmatrix} (\gamma_g u_g)_{g \in \mathcal{G}_E} \\ 0 \end{pmatrix} - X^\top X_E \widehat{\beta}_E - N_E + \begin{pmatrix} (\lambda_g u_g)_{g \in \mathcal{G}_E} \\ (\lambda_g z_g)_{g \in -\mathcal{G}_E} \end{pmatrix}.$$

Note, the term $\begin{pmatrix} (\lambda_g u_g)_{g \in \mathcal{G}_E}^\top & (\lambda_g z_g)_{g \in -\mathcal{G}_E}^\top \end{pmatrix}^\top$ is the subgradient of the ℓ_2 -norm Group LASSO penalty at the solution, where z_g is a vector of variables satisfying

$$\|z_g\|_2 < 1$$

for each non-selected group.

We collect the optimization variables below:

$$\widehat{\gamma} = (\gamma_g : g \in \mathcal{G}_E)^\top \in \mathbb{R}^{|\mathcal{G}_E|},$$

$$\widehat{\mathcal{U}} = \{u_g : g \in \mathcal{G}_E\},$$

$$\widehat{\mathcal{Z}} = \{z_g : g \in -\mathcal{G}_E\},$$

denoting their corresponding instances by γ , \mathcal{U} and \mathcal{Z} . Letting $\text{diag}(\cdot)$ operate on an ordered collection of matrices and return the corresponding block diagonal matrix, we fix $U = \text{diag}\left((u_g)_{g \in \mathcal{G}_E}\right)$. Then, define

$$\phi_{\hat{\beta}_E}(\hat{\gamma}, \hat{\mathcal{U}}, \hat{\mathcal{Z}}) = A\hat{\beta}_E + B(\hat{\mathcal{U}})\hat{\gamma} + c(\hat{\mathcal{U}}, \hat{\mathcal{Z}}), \quad (10)$$

where

$$A = -X^\top X_E, \quad B = X^\top X_E U, \quad c = -N_E + \left((\lambda_g u_g)_{g \in \mathcal{G}_E}^\top \quad (\lambda_g z_g)_{g \in -\mathcal{G}_E}^\top \right)^\top.$$

Finally, we set our conditioning event to be

$$\mathcal{A}_E = \{\hat{E} = E, \hat{\mathcal{U}} = \mathcal{U}, \hat{\mathcal{Z}} = \mathcal{Z}\},$$

clearly a more refined event than observing the active variables.

Remark 3.1. *Despite the additional conditioning encoded within the event \mathcal{A}_E , our empirical analyses in Section 6 provide abundant evidence that the precise correction we apply by conditioning upon this event is only at a very minimal price when compared with naive inference.*

Theorem 3.1 gives an exact expression for the adjustment factor based on a change of variables:

$$\omega \rightarrow (\hat{\gamma}, \hat{\mathcal{U}}, \hat{\mathcal{Z}}), \quad \text{where } (\hat{\gamma}, \hat{\mathcal{U}}, \hat{\mathcal{Z}}) = \phi_{\hat{\beta}_E}^{-1}(\omega), \quad (11)$$

derived upon inverting (10). For each $g \in \mathcal{G}_E$, we construct the orthonormal basis completion for u_g , which we will denote by $\bar{U}_g \in \mathbb{R}^{|g| \times |g|-1}$. Further, $v > t$ for $v \in \mathbb{R}^k$ and $t \in \mathbb{R}$ simply means that the inequality holds in a coordinate-wise sense.

Theorem 3.1. *Define the following matrices*

$$\begin{aligned} \bar{U} &= \text{diag}\left((\bar{U}_g)_{g \in \mathcal{G}_E}\right), \quad \Gamma = \text{diag}\left((\hat{\gamma}_g I_{|g|-1})_{g \in \mathcal{G}_E}\right), \quad \Lambda = \text{diag}\left((\lambda_g I_{|g|})_{g \in \mathcal{G}_E}\right), \\ \Sigma^* &= (B^\top \Omega^{-1} B)^{-1}, \quad A^* = -\Sigma^* B^\top \Omega^{-1} A, \quad b^* = -\Sigma^* B^\top \Omega^{-1} c. \end{aligned}$$

Then, we have

$$\begin{aligned} \mathbb{P}(\mathcal{A}_E \mid \beta_E) \propto \int \int L(\beta_E; \hat{\beta}_E) \exp \left\{ -\frac{1}{2}(\hat{\gamma} - A^* \hat{\beta}_E - b^*)^\top (\Sigma^*)^{-1} (\hat{\gamma} - A^* \hat{\beta}_E - b^*) \right\} \\ \times J_{\phi_{\hat{\beta}_E}}(\hat{\gamma}; \mathcal{U}, \mathcal{Z}) \cdot \mathbf{1}(\hat{\gamma} > 0) d\hat{\beta}_E d\hat{\gamma}, \end{aligned}$$

where

$$J_{\phi_{\hat{\beta}_E}}(\hat{\gamma}; \mathcal{U}, \mathcal{Z}) = \det(\Gamma + \bar{U}^\top (X_E^\top X_E)^{-1} \Lambda \bar{U}). \quad (12)$$

In Theorem 3.1, $J_{\phi_{\hat{\beta}_E}}(\hat{\gamma}; \mathcal{U}, \mathcal{Z})$ represents the Jacobian associated with the change of variables $\phi_{\hat{\beta}_E}(\cdot)$. Noticing the dependence of the function in (12) on $\hat{\gamma}$ and the realized value \mathcal{U} , we will call this as $J_\phi(\cdot; \mathcal{U})$. Clearly, the nontrivial function in our adjustment factor is the function, $J_\phi(\cdot; \mathcal{U})$. The non-affine geometry we set out to analyze in our adjustment factor is now equivalently expressed as simple support constraints on the sizes of the selected groups, along with the Jacobian from the change of variables.

In the special case where the design matrix of the selected model is orthogonal, the otherwise complex Jacobian takes a reduced form; see Corollary 3.1.

Corollary 3.1. *Suppose $X_E^\top X_E = I_{|E|}$. Then*

$$J_\phi(\gamma; \mathcal{U}) = \prod_{g \in \mathcal{G}_E} (\gamma_g + \lambda_g)^{(|g|-1)}.$$

The proof of Corollary 3.1 is a direct calculation based on (12) and is omitted. Further, it is easy to note when all the group sizes are exactly equal to 1, the Jacobian function dissolves as a constant. This is consistent with our expectations since the Group LASSO objective agrees with the canonical LASSO in the case of atomic groups.

3.2 Approximating the selection-informed posterior

Plugging in the adjustment factor from Theorem 3.1 into (7) yields our selection-informed posterior. Computing the theoretical value of this precise correction through conditioning

cannot however be handled directly. Instead, approximations aligned along moderate-deviations type bounds [Panigrahi et al., 2016, 2017] replace the exact expressions for LASSO-type problems admitting an affine selection geometry. In dealing with group-sparse models after learning the sparsity structure from our data, a no longer ignorable Jacobian function encountered in the adjustment factor demands particular attention for computationally amenable methods. Our prime focus thus shifts towards facilitating compact expressions for the centerpiece of our framework, the selection-informed posterior.

Motivated by a generalized version of the Laplace approximation [Wong, 2001, Inglot and Majerski, 2014], Theorem 3.2 relies on an approximate form for the adjustment factor stated below:

$$\begin{aligned}
\mathbb{P}(\mathcal{A}_E \mid \beta_E) &\propto \int \int L(\beta_E; \hat{\beta}_E) \exp \left\{ -\frac{1}{2}(\hat{\gamma} - A^* \hat{\beta}_E - b^*)^\top (\Sigma^*)^{-1} (\hat{\gamma} - A^* \hat{\beta}_E - b^*) \right\} \\
&\quad \times J_\phi(\hat{\gamma}; \mathcal{U}) \mathbf{1}(\hat{\gamma} > 0) d\hat{\beta}_E d\hat{\gamma} \\
&\approx C \exp \left(-\frac{1}{2}(\beta_E^* - \beta_E)^\top \Sigma_E^{-1} (\beta_E^* - \beta_E) - \frac{1}{2}(\gamma^* - A^* \beta_E^* - b^*)^\top (\Sigma^*)^{-1} (\gamma^* - A^* \beta_E^* - b^*) \right. \\
&\quad \left. - \text{Barr}(\gamma^*) \right) \cdot J_\phi(\gamma^*; \mathcal{U});
\end{aligned} \tag{13}$$

C is a constant free of β_E . In computing (13), β_E^* and γ^* are optimizers for the problem

$$\text{minimize}_{\tilde{\beta}_E, \tilde{\gamma}} \left\{ \frac{1}{2}(\tilde{\beta}_E - \beta_E)^\top \Sigma_E^{-1} (\tilde{\beta}_E - \beta_E) + \frac{1}{2}(\tilde{\gamma} - A^* \tilde{\beta}_E - b^*)^\top (\Sigma^*)^{-1} (\tilde{\gamma} - A^* \tilde{\beta}_E - b^*) + \text{Barr}(\tilde{\gamma}) \right\};$$

$\text{Barr}(\cdot)$ takes value ∞ when the support constraints are violated and reflects a smaller penalty for values of $\tilde{\gamma}$ farther away from the boundary of the selection region. We make our choice of barrier penalty explicit in our empirical implementations (Section 6).

Leading to a pliable deployment of gradient-based samplers at large, the following result provides us with a surrogate selection-informed posterior and the associated gradient using the approximation for the adjustment factor in (13). We establish large sample concentra-

tion theory for the resulting posterior later, centering the discussion around our methods in the current section.

Theorem 3.2. *Define the optimization problem*

$$\gamma^* = \underset{\gamma}{\operatorname{argmin}} \frac{1}{2}(\gamma - \bar{P}\beta_E - \bar{q})^\top (\bar{\Sigma})^{-1}(\gamma - \bar{P}\beta_E - \bar{q}) + \operatorname{Barr}(\gamma); \quad (14)$$

$\bar{\Sigma} = \Sigma^* + A^* \Sigma_E (A^*)^\top$, $\bar{P} = \bar{\Sigma}(\Sigma^*)^{-1} A^* (\Sigma_E^{-1} + (A^*)^\top (\Sigma^*)^{-1} A^*)^{-1} \Sigma_E^{-1}$, $\bar{q} = b^*$. Let M_g denote the set of $|g| - 1$ diagonal indices of Γ^* corresponding to group g , and let

$$J^* = \left(\sum_{i \in M_g} [(\Gamma^* + \bar{U}^\top (X_E^\top X_E)^{-1} \Lambda \bar{U})^{-1}]_{ii} \right)_{g \in \mathcal{G}_E} \in \mathbb{R}^{|\mathcal{G}_E|}, \quad \Gamma^* = \operatorname{diag} \left((\gamma_g^* I_{|g|-1})_{g \in \mathcal{G}_E} \right).$$

Then, the logarithm of our surrogate selection-informed posterior is given by

$$\begin{aligned} \log \pi(\beta_E) + \log L(\beta_E; \hat{\beta}_E) + \frac{1}{2}(\gamma^* - \bar{P}\beta_E - \bar{q})^\top (\bar{\Sigma})^{-1}(\gamma^* - \bar{P}\beta_E - \bar{q}) + \operatorname{Barr}(\gamma^*) \\ - \log J_\phi(\gamma^*; \mathcal{U}), \end{aligned} \quad (15)$$

ignoring additive constants. Further, the gradient of the (log) posterior in (15) equals

$$\begin{aligned} \nabla \log \pi(\beta_E) + \Sigma_E^{-1}(\hat{\beta}_E - \beta_E) + \bar{P}^\top (\bar{\Sigma})^{-1} \left\{ \bar{P}\beta_E + \bar{q} - \gamma^* \right. \\ \left. - (\bar{\Sigma}^{-1} + \nabla^2 \operatorname{Barr}(\gamma^*))^{-1} J^* \right\}. \end{aligned} \quad (16)$$

Remark 3.2. *Focusing on (15) and (16) for the surrogate expressions, a take-away from Theorem 3.2 is that we solve a much lower dimensional optimization problem for selection-informed inference. Precisely, the dimension of the problem calculated for the adjustment factor equals the number of groups we select post (1).*

An alternate approximation for (13) is given by

$$\begin{aligned} C \exp \left(-\frac{1}{2}(\beta_E^* - \beta_E)^\top \Sigma_E^{-1}(\beta_E^* - \beta_E) - \frac{1}{2}(\gamma^* - A^* \beta_E^* - b^*)^\top (\Sigma^*)^{-1}(\gamma^* - A^* \beta_E^* - b^*) \right. \\ \left. - \operatorname{Barr}(\gamma^*) + \log J_\phi(\gamma^*; \mathcal{U}) \right), \end{aligned}$$

the usual Laplace approximation where γ^* and β_E^* are obtained by solving

$$\begin{aligned} \text{minimize}_{\tilde{\beta}_E, \tilde{\gamma}} \left\{ \frac{1}{2}(\tilde{\beta}_E - \beta_E)^\top \Sigma_E^{-1}(\tilde{\beta}_E - \beta_E) + \frac{1}{2}(\tilde{\gamma} - A^* \tilde{\beta}_E - b^*)^\top (\Sigma^*)^{-1}(\tilde{\gamma} - A^* \tilde{\beta}_E - b^*) \right. \\ \left. + \text{Barr}(\tilde{\gamma}) - \log J_\phi(\tilde{\gamma}; \mathcal{U}) \right\}. \end{aligned} \quad (17)$$

Remark 3.3. Problem (17) deviates from our current formulation (14) in terms of the part the (log) Jacobian term plays in determining the mode of the optimization. We opt specifically for a generalized formulation of the Laplace approximation to compute the Jacobian only once at the mode of (14) for increased computational efficiency, obtaining our selection-informed posterior and the gradient associated with it.

4 Generalization to Other Grouped Sparsities

Our exposition thus far describes inference in group-sparse linear models under a partition of the covariates into disjoint groups of variables. We now generalize our selection-informed methods to learning algorithms which target other forms of grouped sparsities and covariate structures. The surrogate posterior we feasibly compute in Theorem 3.2 relies on the matrices A^* , b^* and Σ^* involved in the quadratic component of our optimization problem (14). Further, the constraints on the sizes of the selected groups are encoded within the barrier penalty and the Jacobian in our calculations is directly tied to our conditioning event \mathcal{A}_E . In each of our case studies below, we appropriately identify the conditioning event and provide the theoretical value of the crucial adjustment factor. Identifying the exact value of the adjustment directly leads us to the surrogate expressions— (15) and (16)—as we see for the Group LASSO.

4.1 Overlapping Group LASSO

We take up the overlapping Group LASSO formulation [Jacob et al., 2009a] in this discussion. This algorithm recovers superposed groups by augmenting the covariate space with

duplicated predictors. Thus, we implement the solver (1) with a randomization variable $\omega^* \in \mathbb{R}^{p^*} \sim N(0, \Omega)$ such that p^* is the number of duplicated covariates. To formalize the setting, we let $X^* \in \mathbb{R}^{n \times p^*}$ denote the augmented matrix of covariates constructed from $X \in \mathbb{R}^{n \times p}$ given that we have prespecified overlapped grouping. Each set of selected covariates E^* in the augmented space maps to a set of selected variables E in the original space by reversing the duplication.

The stationary mapping for the overlapping Group LASSO with augmented matrix X^* and randomization ω^* is given by

$$\omega^* = X^{*\top} X^* \begin{pmatrix} (\gamma_g^* u_g^*)_{g \in \mathcal{G}_{E^*}} \\ 0 \end{pmatrix} - X^{*\top} X_E \hat{\beta}_E - N_E + \begin{pmatrix} (\lambda_g u_g^*)_{g \in \mathcal{G}_{E^*}} \\ (\lambda_h z_h^*)_{h \in -\mathcal{G}_{E^*}} \end{pmatrix} \quad (18)$$

where $\hat{\beta}_E$ and $N_E = (X^*)^\top (y - X_E \hat{\beta}_E)$ are the refitted and the ancillary statistics in our selected model (cf. (3)). Sticking with our notations,

$$\hat{\gamma}^* = (\gamma_g^* : g \in \mathcal{G}_{E^*})^\top, \quad \hat{\mathcal{U}}^* = \{u_g^* : g \in \mathcal{G}_{E^*}\},$$

represent a polar decomposition of the overlapping Group LASSO solution; let $U^* = \text{diag} \left((u_g^*)_{g \in \mathcal{G}_{E^*}} \right)$. Finally,

$$\mathcal{Z}^* = \{z_g^* : g \in -\mathcal{G}_{E^*}\}$$

are the subgradient variables from the Group LASSO penalty for the non-selected groups in the augmented predictor space.

The conditioning event we study for an analytically feasible selection-informed posterior is given by

$$\mathcal{A}_{E^*} = \{\hat{E}^* = E^*, \hat{\mathcal{U}}^* = \mathcal{U}^*, \hat{\mathcal{Z}}^* = \mathcal{Z}^*\}.$$

We then recover an expression for the adjustment factor along the lines of Theorem 3.1 based on the matrices

$$A = -(X^*)^\top X_E, B = (X^*)^\top X_{E^*}^* U^*, c = -N_E + \left((\lambda_g u_g^*)_{g \in \mathcal{G}_E}^\top \quad (\lambda_g z_g^*)_{g \in -\mathcal{G}_E}^\top \right)^\top. \quad (19)$$

Proposition 4.1. *Define the following matrices*

$$\begin{aligned}\bar{U}^* &= \text{diag} \left((\bar{U}_g^*)_{g \in \mathcal{G}_{E^*}} \right), \Gamma^* = \text{diag} \left((\hat{\gamma}_g^* I_{|g|})_{g \in \mathcal{G}_{E^*}} \right), \Lambda = \text{diag} \left((\lambda_g I_{|g|})_{g \in \mathcal{G}_{E^*}} \right) \\ \Sigma^* &= (B^\top \Omega^{-1} B)^{-1}, A^* = -\Sigma^* B^\top \Omega^{-1} A, b^* = -\Sigma^* B^\top \Omega^{-1} c,\end{aligned}$$

dependent on the objects in (19). Then, $\mathbb{P}(\mathcal{A}_{E^*} \mid \beta_E)$ is proportional to

$$\begin{aligned}\int \int L(\beta_E; \hat{\beta}_E) \exp \left\{ -\frac{1}{2} (\hat{\gamma}^* - A^* \hat{\beta}_E - b^*)^\top (\Sigma^*)^{-1} (\hat{\gamma}^* - A^* \hat{\beta}_E - b^*) \right\} \\ \times J_{\phi^*}(\hat{\gamma}^*; \mathcal{U}^*) \cdot \mathbf{1}(\hat{\gamma}^* > 0) d\hat{\beta}_E d\hat{\gamma}^*,\end{aligned}$$

where

$$J_{\phi^*}(\hat{\gamma}^*; \mathcal{U}^*) = \det \left(((X_{E^*}^*)^\top X_{E^*}^* \Gamma^* + \Lambda) \bar{U}^* \quad (X_{E^*}^*)^\top X_{E^*}^* U^* \right). \quad (20)$$

Notice, since X^* contains overlapping groups, the matrix $(X_{E^*}^*)^\top X_{E^*}^*$ may not be invertible. Thus, in comparison to Theorem 3.1, (20) provides a different expression for the Jacobian function involving the sizes of the selected groups of variables. This value is obtained from (34) in the derivation of the adjustment factor when there are no overlaps in the groups, where we simply replace the original design with the augmented version.

Remark 4.1. *In solving (1), one may introduce a ridge penalty $\epsilon \|\beta\|_2^2/2$, where ϵ is a small positive number. This will in turn lead to (19) with*

$$B = \begin{bmatrix} (X_E^*)^\top X_{E^*}^* + \epsilon \cdot I_{E^*} \\ (X_{-E^*})^\top X_{E^*}^* \end{bmatrix} U^*.$$

This results in the following Jacobian

$$J_{\phi^*}(\hat{\gamma}^*; \mathcal{U}^*) = \det(\Gamma^* + (\bar{U}^*)^\top ((X_{E^*}^*)^\top X_{E^*}^* + \epsilon \cdot I_{E^*})^{-1} \Lambda \bar{U}^*)$$

where the ridge parameter can specifically be used to counter the collinearity in the augmented predictor matrix.

4.2 Standardized Group LASSO

An alternate treatment to the Group LASSO objective is popularly applied in problems with correlated covariates when a within-group orthonormality is desired. The learning algorithm proposed by [Simon and Tibshirani \[2012\]](#) addresses the selection of groups in the presence of such correlations via a modification to the Group LASSO penalty. Equivalently, the canonical objective (1) is reparameterized in the standardized formulation; for each submatrix X_g containing the predictors in group $g \in \mathcal{G}$, the quadratic loss function is given by

$$\|y - \sum_g X_g \beta_g\|_2^2 = \|y - \sum_g W_g \theta_g\|_2^2, \quad (21)$$

$X_g = W_g R_g$ for W_g , an orthonormal matrix and R_g , an invertible matrix and $\theta_g = R_g \beta_g$ is the reparameterized vector. The standardized Group LASSO now optimizes the Group LASSO objective in terms of θ rather than β :

$$\hat{\theta}^{(\mathcal{G})} = \operatorname{argmin}_{\theta} \left\{ \frac{1}{2} \|y - \sum_{g \in \mathcal{G}} W_g \theta_g\|_2^2 + \sum_{g \in \mathcal{G}} \lambda_g \|\theta_g\|_2 - \omega^\top \theta \right\}. \quad (22)$$

The original parameters of interest are then estimated by $R_g^{-1} \hat{\theta}^{(\mathcal{G})}$. The selected set of groups E comprise of groups with non-zero coordinates in $\hat{\theta}^{(\mathcal{G})}$ post solving (22).

Letting $W \in \mathbb{R}^{n \times p}$ be the column-wise concatenation of the standardized groups of covariates W_g , the stationary mapping for the Standardized Group LASSO is given by

$$\omega = W^\top W \begin{pmatrix} (\gamma_g u_g)_{g \in \mathcal{G}_E} \\ 0 \end{pmatrix} - W^\top X_E \hat{\beta}_E - N_E + \begin{pmatrix} (\lambda_g u_g)_{g \in \mathcal{G}_E} \\ (\lambda_h z_h)_{h \in -\mathcal{G}_E} \end{pmatrix}; \quad (23)$$

$\hat{\beta}_E$ is our usual refitted statistic and $N_E = W^\top (Y - X_E \hat{\beta}_E)$. Consistent with our approach, a polar decomposition of the (nonzero) Standardized Group LASSO solution $\hat{\theta}^{(\mathcal{G})}$ is represented via

$$\gamma = (\gamma_g : g \in \mathcal{G}_E), \mathcal{U} = \{u_g : g \in \mathcal{G}_E\}.$$

Sticking to our usual notations, recall

$$\mathcal{Z} = \{z_g : g \in -\mathcal{G}_E\}$$

are the subgradient variables for the non-selected groups. Setting

$$\begin{aligned} \mathcal{A}_E &= \{\hat{E} = E, \hat{\mathcal{U}} = \mathcal{U}, \hat{\mathcal{Z}} = \mathcal{Z}\}, \\ A &= -W^\top X_E, B = W^\top W_E U, c = -N_E + \left((\lambda_g u_g)_{g \in \mathcal{G}_E}^\top \quad (\lambda_g z_g)_{g \in -\mathcal{G}_E}^\top \right)^\top, \end{aligned} \quad (24)$$

we present the key adjustment factor analogous to Theorem 3.1 after a change of variables.

Proposition 4.2. *Consider the following matrices*

$$\begin{aligned} \bar{U} &= \text{diag} \left((\bar{U}_g)_{g \in \mathcal{G}_E} \right), \Gamma = \text{diag} \left((\hat{\gamma}_g I_{|g|-1})_{g \in \mathcal{G}_E} \right), \Lambda = \text{diag} \left((\lambda_g I_{|g|})_{g \in \mathcal{G}_E} \right), \\ \Sigma^* &= (B^\top \Omega^{-1} B)^{-1}, A^* = -\Sigma^* B^\top \Omega^{-1} A, b^* = -\Sigma^* B^\top \Omega^{-1} c. \end{aligned}$$

We then have

$$\begin{aligned} \mathbb{P}(\mathcal{A}_E \mid \beta_E) &\propto \int \int L(\beta_E; \hat{\beta}_E) \exp \left\{ -\frac{1}{2} (\hat{\gamma} - A^* \hat{\beta}_E - b^*)^\top (\Sigma^*)^{-1} (\hat{\gamma} - A^* \hat{\beta}_E - b^*) \right\} \\ &\quad \times J_\phi(\hat{\gamma}; \mathcal{U}) \cdot \mathbf{1}(\hat{\gamma} > 0) d\hat{\beta}_E d\hat{\gamma}; \\ J_\phi(\hat{\gamma}; \mathcal{U}) &= \det(\Gamma + \bar{U}^\top (W_E^\top W_E)^{-1} \Lambda \bar{U}). \end{aligned}$$

4.3 Sparse Group LASSO

We turn our attention to a structural assumption on the groups of variables when sparsity exists both across and within groups. The Sparse Group LASSO [Friedman et al., 2010] produces solutions that are sparse at both the group level and the individual level within selected groups by deploying the Group LASSO penalty along with the usual ℓ_1 penalty. A randomized formulation of the Sparse Group LASSO is thus given by

$$\underset{\beta}{\operatorname{argmin}} \left\{ \frac{1}{2} \|y - X\beta\|_2^2 + \sum_g \lambda_g \|\beta_g\|_2 + \lambda_0 \|\beta\|_1 - \omega^\top \beta \right\}; \quad (25)$$

the sum over g forms a non-overlapping partition of the predictors. Notice, this criterion may be viewed a special case of the overlapping Group LASSO where each predictor i appears in a group $g \in \{1, \dots, G\}$, as well as in its own individual group.

Setting up notations, let \mathcal{G}_E denote the set of selected groups, and $-\mathcal{G}_E$ denote its complement; let T_g denote the selected predictors in group g , and $-T_g$ the corresponding complement. Finally, we define

$$\check{E} = \cup_{g \in \mathcal{G}_E} T_g,$$

the set of selected predictors in the selected groups which parameterize our selected model.

We write the stationary mapping for the Sparse Group LASSO below

$$\begin{aligned} \omega = X^\top X \begin{pmatrix} (\gamma_g u_g)_{g \in \mathcal{G}_E} \\ 0 \end{pmatrix} - X^\top X_{\check{E}} \hat{\beta}_{\check{E}} - N_{\check{E}} + \begin{pmatrix} (\lambda_g u_g)_{g \in \mathcal{G}_E} \\ (\lambda_h z_h)_{h \in -\mathcal{G}_E} \end{pmatrix} \\ + \lambda_0 \left(\begin{pmatrix} (s_j)_{j \in T_g} \\ (s_j)_{j \in -T_g} \end{pmatrix}_{g \in \mathcal{G}} \right) \end{aligned} \quad (26)$$

where $\hat{\beta}_{\check{E}}$ and $N_{\check{E}}$ are defined as per projections according to the selected model. Recall, γ , \mathcal{U} and \mathcal{Z} are consistent in their definition in terms of the groups we select after solving (1). In addition, the subgradient variables from the ℓ_1 penalty are represented by s_j , with $s_j = \text{sign}(\hat{\beta}_j^{(\mathcal{G})})$ for $j \in \check{E}$, and $|s_j| < 1$ for $j \in -\check{E}$. We collect these scalar variables into the two sets, $\mathcal{S}_{\mathcal{G}_E}$ and $\mathcal{S}_{-\mathcal{G}_E}$, depending on whether the predictor is in a selected group. For non-selected predictors in selected groups, the corresponding entry of u_g is zero. That is, we can interpret u_g as a unit vector with the same dimension as the selected part of group g , denoting it by $\check{u}_g = (u_{g,j} : j \in T_g)^\top \in \mathbb{R}^{|T_g|}$. Set $\check{U} = \text{diag}((\check{u}_g)_{g \in \mathcal{G}_E})$.

Define the selection event

$$\mathcal{A}_{\check{E}} = \{\hat{E} = \check{E}, \hat{\mathcal{U}} = \mathcal{U}, \hat{\mathcal{Z}} = \mathcal{Z}, \hat{\mathcal{S}}_{\mathcal{G}_E} = \mathcal{S}_{\mathcal{G}_E}, \hat{\mathcal{S}}_{-\mathcal{G}_E} = \mathcal{S}_{-\mathcal{G}_E}\}, \quad (27)$$

$$A = -X^\top X_{\check{E}}, B = X^\top X_{\check{E}} \check{U}, c = -N_{\check{E}} + \begin{pmatrix} (\lambda_g u_g)_{g \in \mathcal{G}_E}^\top & (\lambda_g z_g)_{g \in -\mathcal{G}_E}^\top \end{pmatrix}^\top + \lambda_0 \left(((s_j)_{j \in g})_{g \in \mathcal{G}} \right)^\top, \quad (28)$$

using the stationary mapping for the learning algorithm under scrutiny. We then recover the following theoretical expression for the adjustment factor for the Sparse Group LASSO.

Proposition 4.3. For each selected group $g \in \mathcal{G}_E$, construct $\bar{U}_g \in \mathbb{R}^{|T_g| \times (|T_g|-1)}$ as the orthonormal basis completion of \check{u}_g . Define the following matrices

$$\bar{U} = \text{diag} \left(\left(\bar{U}_g \right)_{g \in \mathcal{G}_E} \right), \Gamma = \text{diag} \left(\left(\gamma_g I_{|T_g|-1} \right)_{g \in \mathcal{G}_E} \right), \Lambda = \text{diag} \left(\left(\lambda_g I_{|T_g|} \right)_{g \in \mathcal{G}_E} \right), \\ \Sigma^* = (B^\top \Omega^{-1} B)^{-1}, A^* = -\Sigma^* B^\top \Omega^{-1} A, b^* = -\Sigma^* B^\top \Omega^{-1} c$$

based upon (28). Then, we have

$$\mathbb{P}(\mathcal{A}_E \mid \beta_E) \propto \int \int L(\beta_E; \hat{\beta}_E) \exp \left\{ -\frac{1}{2} (\hat{\gamma} - A^* \hat{\beta}_E - b^*)^\top (\Sigma^*)^{-1} (\hat{\gamma} - A^* \hat{\beta}_E - b^*) \right\} \\ \times J_\phi(\hat{\gamma}; \mathcal{U}) \mathbf{1}(\gamma > 0) d\hat{\beta}_E d\gamma.$$

where

$$J_\phi(\hat{\gamma}; \mathcal{U}) = \det(\Gamma + \bar{U}^\top (X_E^\top X_E)^{-1} \Lambda \bar{U}).$$

5 Large sample theory: selection-informed posterior

In this section, we establish statistical credibility for our surrogate selection-informed posterior under a fixed p and growing n regime. Introducing the dependence of our statistics on the sample size, we denote the naive joint likelihood as follows

$$L_n(\beta_{n,E}; \hat{\beta}_{n,E}, \omega_n) \propto \exp \left\{ -\frac{n}{2} (\beta_{n,E} - \hat{\beta}_{n,E})^\top \Sigma_E^{-1} (\beta_{n,E} - \hat{\beta}_{n,E}) - \frac{n}{2} \omega_n^\top \Omega^{-1} \omega_n \right\},$$

and let $L_n(\beta_{n,E}; \hat{\beta}_{n,E})$ be the marginal likelihood based upon the least squares estimate. Now, let $\ell_{n,S}(\cdot; \hat{\beta}_{n,E} \mid N_{n,E})$ represent the surrogate (log) selection-informed counterpart in Theorem 3.2, which in our setup equals :

$$\log L_n(\beta_{n,E}; \hat{\beta}_{n,E}) + \frac{n}{2} (\gamma_n^* - \bar{P} \beta_{n,E} - \bar{q}/\sqrt{n})^\top (\bar{\Sigma})^{-1} (\gamma_n^* - \bar{P} \beta_{n,E} - \bar{q}/\sqrt{n}) \\ + \text{Barr}(\sqrt{n} \gamma_n^*) - \log J_\phi(\sqrt{n} \gamma_n^*; \mathcal{U}),$$

(up to an additive constant in $\beta_{n,E}$), relying upon the optimizer

$$\gamma_n^* = \underset{\gamma}{\operatorname{argmin}} \frac{n}{2} (\gamma - \bar{P}\beta_{n,E} - \bar{q}/\sqrt{n})^\top (\bar{\Sigma})^{-1} (\gamma - \bar{P}\beta_{n,E} - \bar{q}/\sqrt{n}) + \operatorname{Barr}(\sqrt{n}\gamma).$$

We consider $\sqrt{n}\beta_{n,E} = b_n\bar{\beta}_E$, where $n^{-1/2}b_n = O(1)$, and $b_n \rightarrow \infty$ as $n \rightarrow \infty$. Define

$$\mathcal{B}(\beta_{n,E}, \delta) = \left\{ z : \|z - \beta_{n,E}\|_2^2 < \delta \right\},$$

a ball of radius δ around our parameter of interest, $\beta_{n,E}$. Appending our surrogate selection-informed likelihood to a prior $\pi(\cdot)$ gives us our selection-informed posterior, and we denote the measure of a set \mathcal{K} with respect to this posterior as follows

$$\Pi_{n,S}(\mathcal{K} \mid \hat{\beta}_{n,E}; N_{n,E}) = \frac{\int_{\mathcal{K}} \pi(z_n) \cdot \exp(\ell_{n,S}(z_n; \hat{\beta}_{n,E} \mid N_{n,E})) \, dz_n}{\int \pi(z_n) \cdot \exp(\ell_{n,S}(z_n; \hat{\beta}_{n,E} \mid N_{n,E})) \, dz_n}. \quad (29)$$

Lastly we use $\mathbb{P}_{n,S}(\cdot)$ in this section to represent the selection-informed probability after conditioning upon our selection event and the ancillary statistic under our parameter of interest, $\beta_{n,E}$.

Our main theoretical result, Theorem 5.1, proves that our surrogate version of the selection-informed posterior concentrates around the true parameter as our sample size grows infinitely large, giving us the rate of contraction of our posterior. This result showcases in particular the frequentist appeal of our proposed Bayesian methodology. We begin with two supporting propositions: (i) Proposition 5.1 proves the convergence of our (approximate) adjustment factor to the exact counterpart when the support constraints for the sizes of the selected groups are restricted to a compact subset; (ii) Proposition 5.2 bounds the curvature of the surrogate (log) selection-informed likelihood around its maximizer. To complete Proposition 5.2, Lemma 1 and Lemma 2 provide supplementary theory to control the asymptotic orders of the gradient and Hessian of the (log) Jacobian in our surrogate selection-informed posterior. We include both these results in Supplementary material C.

Proposition 5.1. *Suppose that*

$$\lim_{n \rightarrow \infty} (b_n)^{-2} \{ \log \mathbb{P}(\sqrt{n}\gamma_n > 0) - \log \mathbb{P}(\sqrt{n}\gamma_n > \bar{q}) \} = 0. \quad (30)$$

Then we have

$$\begin{aligned} \lim_{n \rightarrow \infty} (b_n)^{-2} \log \mathbb{P}(0 < \sqrt{n}\gamma_n < b_n \bar{Q} \cdot \mathbf{1}_{|E|} + \bar{q}) + (b_n)^{-2} \text{Barr}(b_n \bar{\gamma}_n^*) - (b_n)^{-2} \log J_\phi(b_n \bar{\gamma}_n^*; \mathcal{U}) \\ + \frac{1}{2}(\bar{\gamma}_n^* - \bar{P}\bar{\beta}_E - (b_n)^{-1}\bar{q})^\top \bar{\Sigma}^{-1}(\bar{\gamma}_n^* - \bar{P}\bar{\beta}_E - (b_n)^{-1}\bar{q}) = 0, \end{aligned}$$

where $\bar{\gamma}_n^$ is defined as follows*

$$\text{argmin}_{\bar{\gamma} < \bar{Q} \cdot \mathbf{1}_{|E|}} \frac{b_n^2}{2} (\bar{\gamma} - \bar{P}\bar{\beta}_E - \bar{q}/b_n)^\top \bar{\Sigma}^{-1} (\bar{\gamma} - \bar{P}\bar{\beta}_E - \bar{q}/b_n) + \text{Barr}(b_n \bar{\gamma}).$$

Remark 5.1. *For a fixed prior $\pi(\cdot)$, we may choose \bar{Q} to be a positive constant in order to consider a sufficiently large compact subset of our selection region that would work for all $\bar{\beta}_E$ in a bounded set of probability close to 1 under our prior. Proposition 5.1 now implies that the our surrogate (log) selection-informed likelihood converges to its exact counterpart which is obtained by plugging in the exact probability of selection, under the parameter sequence $\beta_{n,E}$, as the sample size grows to ∞ .*

Proposition 5.1 and the above remark together motivate the approximation for the adjustment factor in Theorem 3.1:

$$\begin{aligned} \exp \left(-\frac{n}{2} (\gamma_n^* - \bar{P}\bar{\beta}_E - \bar{q}/\sqrt{n})^\top \bar{\Sigma}^{-1} (\gamma_n^* - \bar{P}\bar{\beta}_E - \bar{q}/\sqrt{n}) \right. \\ \left. - \text{Barr}(\sqrt{n}\gamma_n^*) + \log J_\phi(\sqrt{n}\gamma_n^*; \mathcal{U}) \right), \end{aligned} \quad (31)$$

by substituting $b_n \bar{\gamma}$ with $\sqrt{n}\gamma$ in the optimization objective of the Proposition.

Proposition 5.2. *Fix $\mathcal{C} \in \mathbb{R}^{|E|}$, a compact set. Define $\hat{\beta}_{n,E}^{\max}$ to be the maximizer of the selection-informed likelihood sequence, $\ell_{n,S}(\cdot; \hat{\beta}_{n,E} \mid N_{n,E})$. Then there exist positive*

constants $C_0 \leq C_1$ and $N \in \mathbb{N}$ such that for any $0 < \epsilon_0 < C_0$,

$$\begin{aligned} -\frac{n}{2}(C_1 + \epsilon_0)\|z_n - \hat{\beta}_{n,E}^{max}\|_2^2 &\leq \ell_{n,S}(z_n; \hat{\beta}_{n,E} \mid N_{n,E}) - \ell_{n,S}(\hat{\beta}_{n,E}^{max}, \hat{\beta}_{n,E} \mid N_{n,E}) \\ &\leq -\frac{n}{2}(C_0 - \epsilon_0)\|z_n - \hat{\beta}_{n,E}^{max}\|_2^2 \end{aligned}$$

for all $n \geq N$ and $z_n \in \mathcal{C}$.

We are now ready to state and prove our main theoretical result on the concentration properties of our selection-informed posterior.

Theorem 5.1. *Fix $\sqrt{n}\delta_n = b_n\delta$. Suppose a prior $\pi(\cdot)$ with compact support \mathcal{C} assigns non-zero probability to $\mathcal{B}(\beta_{n,E}, \delta) \subset \mathcal{C}$ for any $\delta > 0$. Further, assume for the associated prior measure $\Pi(\cdot)$ that*

$$\lim_{n \rightarrow \infty} \exp(-b_n^2 \delta^2 K/2) / \Pi(\mathcal{B}(\beta_{n,E}, \kappa \delta_n)) = 0$$

for any $K > 0$ and $\kappa \in (0, 1)$. Then, the following convergence must hold for any $\epsilon > 0$, $\delta > 0$:

$$\mathbb{P}_{n,S} \left(\Pi_{n,S} \left(\mathcal{B}^c(\beta_{n,E}, \delta_n) \mid \hat{\beta}_{n,E}; N_{n,E} \right) \leq \epsilon \right) \rightarrow 1 \text{ as } n \rightarrow \infty.$$

We next investigate the performance of our selection-informed methodology in a wide range of empirical experiments.

6 Empirical investigations

We first provide the details of a generic implementation of our sampler in Section 6.1, to generate draws from the surrogate selection-informed posteriors. Then, in Section 6.2, we undertake numerical simulations under the canonical Group LASSO (1), and compare our proposal with naive inference and two variants of data splitting. In Section 6.3, we highlight how our method can be adapted for extensions to other grouped sparsities discussed in

Section 4. We conclude with an application of our methodology to a human neuroimaging dataset in Section 6.4, where we leverage specifically the ability of our Bayesian machinery to infer about context-relevant targets.

6.1 Generic implementation

We describe our generic sampling-based scheme for selection-informed inference below, that we call “PoSI” in our empirical analyses. Consider solving the randomized Group LASSO formulation in (1) for now. Then deploying the surrogate expressions for the posterior we identify in Theorem 3.2, a (gradient-based) Langevin sampler takes a noisy step along the gradient of our posterior (16) at each draw. That is, each sample is updated in our implementations as:

$$\beta_E^{(K+1)} = \beta_E^{(K)} + \eta S \nabla \log \tilde{\pi}_S(\beta_E^{(K)}) + \sqrt{2\eta} \epsilon^{(K)}, \quad (32)$$

where $\eta > 0$ is a predetermined step size, $\tilde{\pi}_S$ denotes our surrogate selection-informed posterior and $\epsilon^{(K)} \sim N(0, S)$, our Gaussian proposal [Ahn et al., 2012, Shang et al., 2015]. In practice, we set $\eta = 1$ and determine S from the inverse of the Hessian of our (negative-log) posterior under a diffuse prior. It bears emphasis that this sampler serves as a representative execution of our methods; more generally, other sampling schemes to deliver inference based upon our selection-informed posterior are certainly possible.

Recall, $|\mathcal{G}_E|$ is the number of groups we recover post selection. Remarkably, every draw in our sampling scheme solves only a $|\mathcal{G}_E|$ -dimensional optimization problem (14). This observation is particularly important from a computational feasibility and efficiency perspective, underscoring that an update based on the posterior utilizes an optimization in dimensions that are much lower than the initial regression size, p .

6.2 Experiments: the canonical Group LASSO

We study the ability of our methods to recover effect sizes of covariates in our group-sparse model with statistical accuracy under varying grouped forms and signal strengths. In all of our experiments with synthetic data, we construct the design X by drawing $n = 500$ rows independently according to $\mathcal{N}_p(0, \Sigma)$; Σ follows an auto-regressive structure with the (i, j) -th entry of the covariance matrix $\Sigma_{(i,j)} = 0.2^{|i-j|}$. For a fixed support and values of β that we set according to a variety of schemes described below; in each case, we have a low, medium, and high signal-to-noise ratio (SNR) variant. Finally, we draw $Y \sim \mathcal{N}_n(X\beta, \sigma^2 I_n)$, a Gaussian group-sparse linear model; we fix $\sigma^2 = 3$ in our experiments. Aligned with [Panigrahi et al., 2016], we use a diffuse prior to assess the frequentist credibility of our Bayesian machinery.

For each realization of the data, we apply four methods: (i) “PoSI”, the selection-informed generic method described in Section 6.1; (ii) “Naive”, the standard inferential tool which uses the refitted least squares estimate and clearly does not adjust for selection; (iii) “Split 1:1”; and (iv) “Split 2:1”. The nominal level for the interval estimates for all methods is set at 90%. When applying the PoSI method, we first solve the Group LASSO (1) with a p -dimensional isotropic Gaussian randomization variable independent of our response; that is, $\omega \sim \mathcal{N}_p(0, \tau^2 \cdot I_p)$ and the ratio of randomization variation to the noise level in our response is set at 0.5 [Panigrahi et al., 2019]. We then use the procedure described in Section 6.1 to obtain draws from the (approximate) posterior. The Naive method first fits the usual Group LASSO (1) with no randomization ($\omega = 0$), to identify the active set E , and then fits $\hat{\beta}_E$ using ordinary least squares restricted to X_E from which we obtain confidence intervals using normal quantiles. The latter two “Split” methods follow the same procedure as the Naive method except that they partition the data at the specified ratio, and apply the non-randomized Group LASSO to the first part to obtain E and then use the second part to fit a linear model restricted to E for interval estimation.

Reporting the lengths and coverages of interval estimates when averaged across 100 simulations, we compare the performance of PoSI with Naive, Split 1:1, and Split 2:1 in three diversified settings:

1. Atomic: In the atomic setting, each covariate is in one group and all the groups are distinct. We select 5 groups (equivalently 5 nonzero variables since each group is a singleton) to be active. This is a special case where the randomized Group LASSO coincides with the randomized LASSO. Thus, our selection-informed methods orient with inference after the LASSO [Panigrahi et al. \[2016\]](#), with this case study primarily serving as a first soundness check.
2. Balanced: In our balanced analysis, we partition our $p = 100$ covariates into 25 groups each of cardinality four. In contrast to the atomic setting, because the group sizes are greater than 1, this results in a nontrivial grouped sparsity imposing a grouped penalty distinct from the usual LASSO. We randomly select three of these candidate groups to be active, and again let each coefficient have a random sign with the same magnitudes.
3. Heterogeneous: In the heterogeneous setting, we allow the groups of covariates to differ in their sizes. Further, our groups of covariates now display heterogeneity in the signal amplitudes both within and between the active groups. We have 3 groups with three predictors each, 4 groups with four predictors each, 5 groups with five predictors each, and 5 groups with ten predictors each. We set one of each of the three-, four-, and five-predictor groups to be active with linearly increasing signal magnitudes and each active coefficient is assigned a random sign.

Results of our four methods in these three settings are summarized in Figures [2](#) and [3](#). Unsurprisingly naive inference does not achieve nominal coverage, calling for selection-informed methods which can correct precisely for the effects of bias from these automated

model selections. In agreement with our expectations, PoSI and data splitting methods achieve the nominal coverage rates. Data splitting does not however borrow residual information from the training samples. The consequence of discarding the training samples is a significantly reduced inferential power which we observe as intervals considerably longer than PoSI after solving the nontrivial group LASSO objective. Noteworthy for the balanced and heterogeneous settings, PoSI provides intervals nearly as short as naive inference. This validates our claim of restoring inferential validity at a very nominal price we pay for the selection-informed nature of our group-sparse models and consolidates Remark 3.1. The gains in power is indeed attributed to an optimal utility of information within our data via a Gaussian randomized framework for our methodology.

6.3 Experiments: generalization to other grouped sparsities

Next, we show how our methods generalize in their application to the overlapping and standardized Group LASSO. As before, all methods proceed by first identifying a model parameterized by the active set E obtained from solving the associated optimizations. Inference proceeds for the selection-informed parameters within these models by using the surrogate posterior we construct through an adjustment factor in Section 4.

For the overlapping Group LASSO, we have 34 groups of four predictors each, but the last feature of the first group is also the first feature of the second group, and so on. As a result, the first and last groups each have three features in no other groups, and all other groups have two features in no other groups, for a total of $p = 103$ features. We take the approach of Jacob et al. [2009b] which involves duplicating overlapping features in order to obtain an augmented design matrix X^* with no overlaps. Because columns are duplicated, the expanded design matrix is rank deficient; we therefore incorporate a (small) ridge term consistent with Remark 4.1 in our learning algorithm. After selecting the active set E^* , we map back to the set of selected variables E in the original space to define our

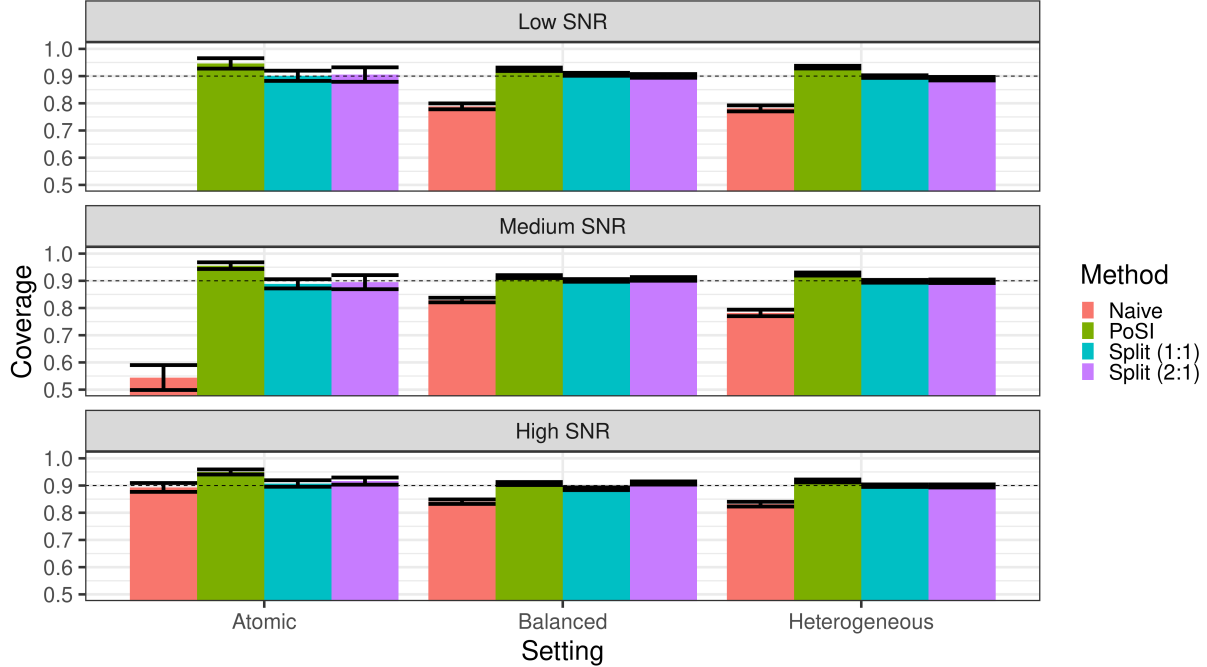


Figure 2: Coverage for experiments under the canonical Group LASSO. A dashed line depicts the nominal 90% coverage rate. Bars depict mean coverage averaged across experimental replications where the method selected a non-empty active set; error bars depict standard errors across experimental replications.

group-sparse model and perform inference for β_E . For the standardized Group LASSO, we use the same setup under the balanced setting in Section 6.2, i.e., our instance involves 25 non-overlapping groups each of size four for a total of $p = 100$ features.

Results of all methods under scrutiny in these two settings are depicted in Figures 4 and 5. Naive inference falls short of nominal coverage; the lengths of these interval estimates give us a benchmark to assess the cost we pay in order to account for selection. Of the remaining methods, all three appear to achieve at least nominal coverage, but PoSI

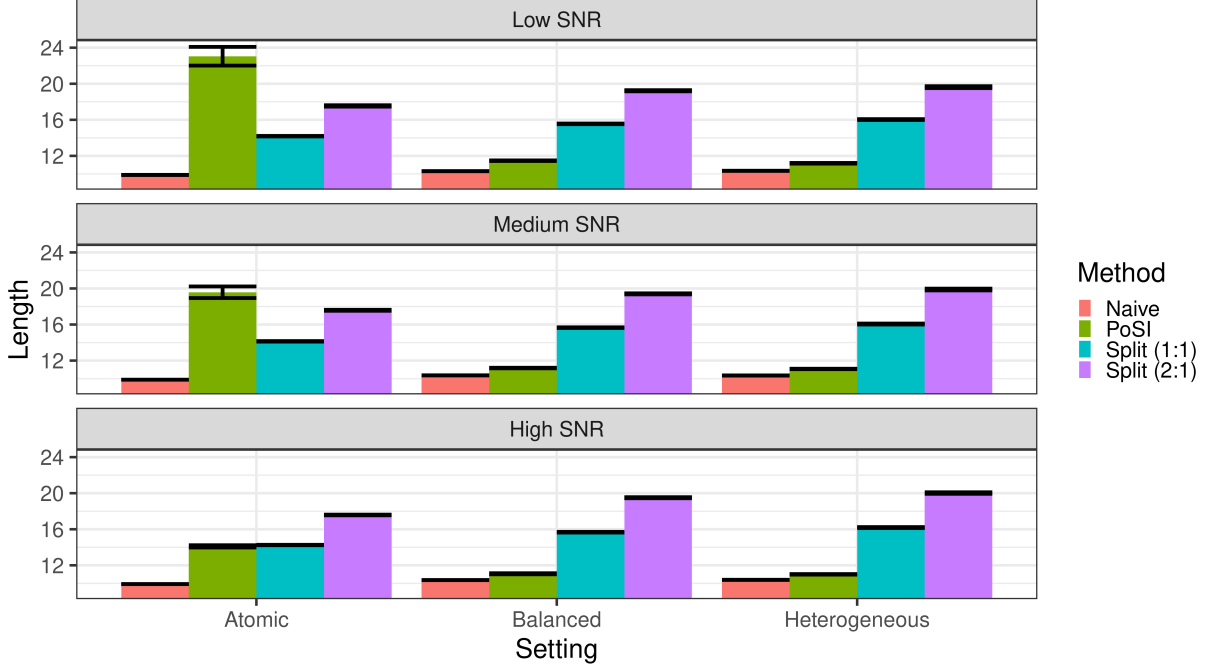


Figure 3: Interval lengths for experiments under the canonical Group LASSO. Bars depict mean interval lengths across experimental replications where the method selected a non-empty active set; error bars depict standard errors across experimental replications.

consistently gives the shortest intervals. The plots yet again highlight a very desirable allocation of information within the available data for selection and subsequent inference.

6.4 Application to Neuroimaging Data

Next, we apply our method to a subset of human neuroimaging data from the Human Connectome Project (HCP) [Van Essen et al., 2013] described in Sripada et al. [2020]. We consider a linear model to predict participant accuracy on a working memory task using brain activity measured at a number of locations in the brain during performance of the task. We group our predictors by brain system and apply the PoSI method described in

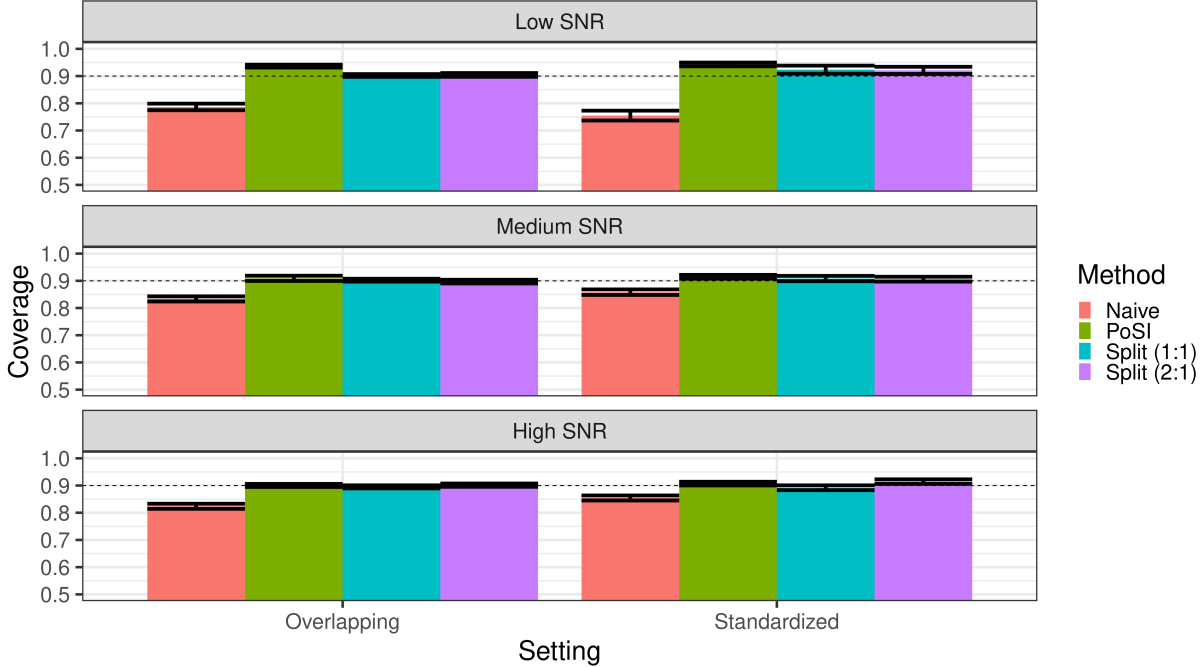


Figure 4: Coverage for experiments under the Overlapping Group LASSO and Standardized Group LASSO. A dashed line depicts the nominal 90% coverage rate. Bars depict mean coverage averaged across experimental replications where the method selected a non-empty active set; error bars depict standard errors across experimental replications.

Section 6.1 to obtain draws from the selection-informed surrogate posterior, which we use to calibrate interval estimates for key functions of the matched coefficients.

The HCP is a landmark study undertaken by a consortium involving Washington University, the University of Minnesota, and Oxford University, and it involved substantial advancement of human neuroimaging methodology and included the collection of several corpora of data which are available to researchers interested in studying brain function and connectivity. We use a subset of 785 participants drawn from the HCP’s “S1200 Release”

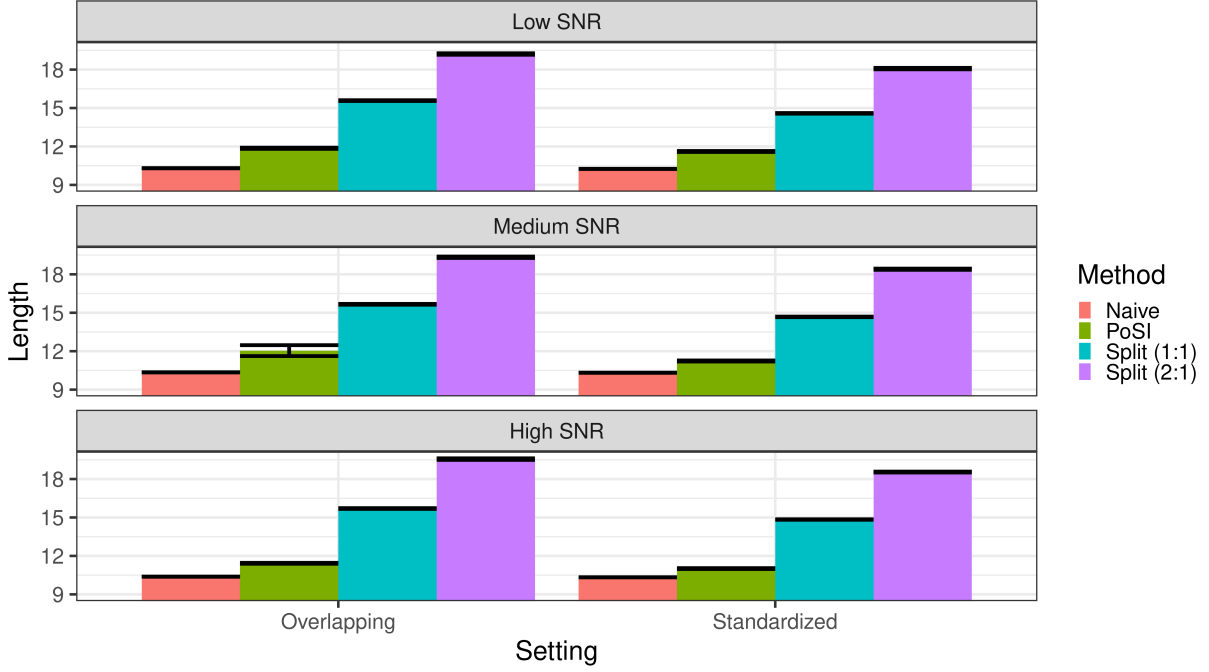


Figure 5: Interval lengths for experiments under the Overlapping Group LASSO and Standardized Group LASSO. Bars depict mean interval lengths across experimental replications where the method selected a non-empty active set; error bars depict standard errors across experimental replications.

which was part of the HCP young adult study [WU-, 2017]. While the HCP data includes a variety of imaging modalities, in the application here we consider both behavioral and functional magnetic resonance imaging (fMRI) data recorded from the “N-back” task, which is summarized below and is described in Barch et al. [2013]. Imaging data is available in preprocessed form after undergoing a processing stream described in Glasser et al. [2013]. This data was used in the recent publication Sripada et al. [2020], and its authors have graciously further processed and shared a subset of this data.

After preliminary processing steps (described in [Glasser et al. \[2013\]](#), [Sripada et al. \[2020\]](#)), the fMRI dataset comprises time courses at potentially hundreds of thousands of “voxels” that are typically each a few cubic millimeters in volume. This yields very high dimensional data, and analysis is sometimes instead performed at the level of “regions of interest” (ROIs), which provide a means of effectively downsampling the data by aggregating information at each ROI, which is a spatially contiguous group of voxels. These ROIs can be defined *a priori* according to one of a variety of atlases, and this aids interpretability and enables comparisons of findings across studies that use the same atlas. We use ROIs as defined by the “Power Parcellation” [[Power et al., 2011](#)]. In addition to being a broadly popular atlas, the Power Parcellation is also noteworthy in that it assigns each of its 264 regions to a “brain system.” The spatial coordinates of the ROIs, as well as their assignment to brain systems, are described in [Power et al. \[2011\]](#). Of the 264 ROIs, 236 are assigned to one of 13 distinct, named brain systems while the remainder are simply labeled “unknown” and in our analysis we use only these 236 positively labeled ROIs as predictors in our regression. Because each of these brain systems is putatively believed to underlie a discrete set of functions (e.g., because they typically coactivate for a given type of task), we partition our predictors into groups by brain system label, and then use the Group LASSO to predict accuracy on the N-back task using data from these 236 ROIs. While inference may be performed at the level of individual ROIs, it is also useful to interrogate effects at a system-wide level. Further averaging all of the ROIs within a single system may be too coarse and obscure useful signal, so the Group LASSO provides a means of allowing each ROI to make a distinct predictive contribution while still performing selection at the interpretable level of entire brain systems.

Brain imaging data was acquired while participants engaged in the “N-back” task [[Barch et al., 2013](#)]. In this task, participants are presented with a sequence of pictures about which they make judgments. There are two different conditions of principle interest, each of which

are presented in blocks. In the 0-back condition, participants simply judge whether each item is the same as the one presented at the beginning of the block. In the 2-back condition, participants judge whether each item is the same as the one two trials previous. As may be intuitively clear, the 2-back condition is appreciably more demanding with respect to working memory. The standardized accuracy of each participant during this task will be our target of prediction y and we will use activity during the task as the predictor X .

A common approach for analyzing fMRI data involves the construction of so-called “contrasts.” Measuring activity during the “2-back” condition would likely indicate activity related to working memory, but it would also include activity indicating many other phenomena such as visual processing, motor activation in order to press buttons to indicate judgments, etc. These phenomena are not of primary interest, so researchers construct a contrast by subtracting the activation during one condition from the activation during another condition. Our contrast of interest is the “2-back” activation minus the “0-back” activation, which is a standard contrast for the N-back task [Barch et al., 2013].

Applying the randomized Group LASSO as described above and setting $\lambda = 25$ results in the selection of two groups: the “Default Mode” system and the “Fronto-parietal Task Control” system. We use the PoSI method to draw samples from the surrogate selection-adjusted posterior. Although not surprising given the overlap between datasets employed, Sripada et al. [2020] found that deactivation in the Default Mode system and activation in the Fronto-parietal Task Control system are a hallmark that indicate the ability of a given task to predict the “General Cognitive Ability” (GCA). The 2-back versus 0-back contrast is identified as being especially useful for predicting GCA. The pattern of activation in the fronto-parietal system and deactivation in the default mode system under general cognitive demands (including working memory) is discussed and reviewed in Sripada et al. [2020].

To highlight the flexibility of our method, we obtain 80%, 90%, and 95% interval estimates for four quantities computed for each selected group: the mean of the coefficients,

the variance of the coefficients, the l_2 -norm of the coefficients, and the maximal magnitude of the coefficients. A frequent challenge in neuroimaging research is determining when data aggregation is appropriate; taken together information about group-wise means and variances enables a researcher to decide whether signal may be safely aggregated or not, whereas the l_2 norm conveys information about the overall importance of the group, and the max conveys information about whether individual regions within that system may be highly predictive. Interval estimates for these quantities are presented in Figure 6.

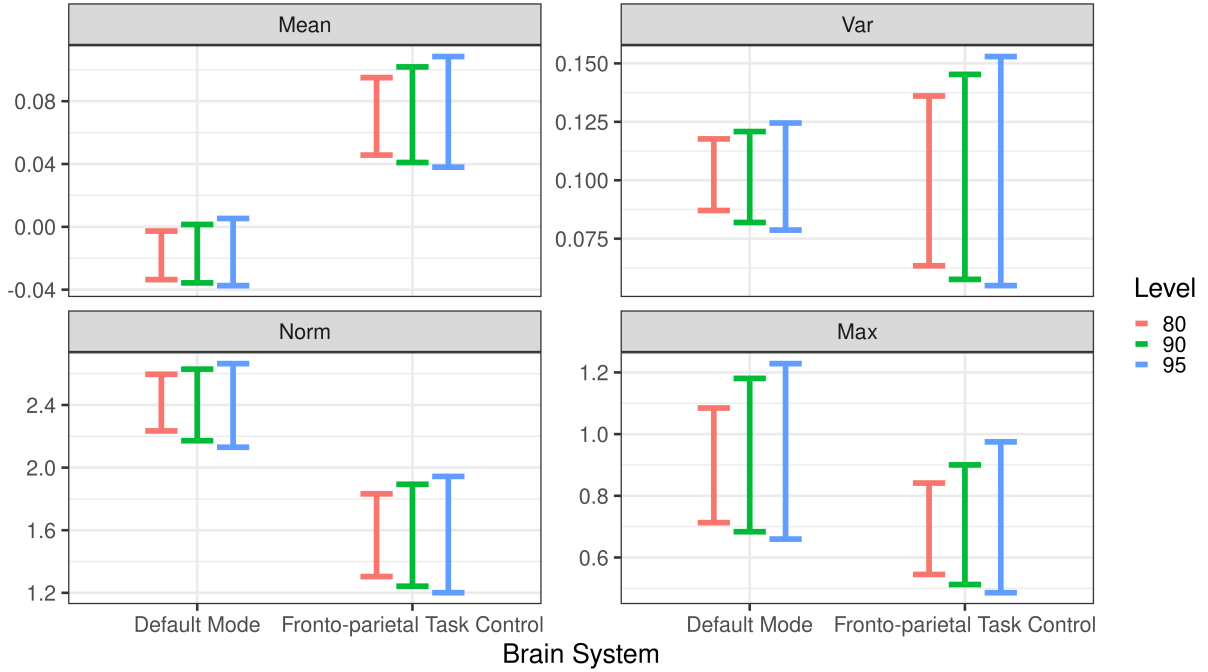


Figure 6: Group-wise interval estimates for two selected brain systems at varying levels for four quantities from human neuroimaging application.

7 Conclusion

In this paper, we provide methods to account for the selection-informed nature of models after solving group-sparse learning algorithms. Deriving conditional inference in these settings is particularly challenging due to a breakdown of an affine geometry associated with the selection event. To this end, our methods offer a distinct way out to deal with the infeasibility of computing truncation regions during retrieval of pivots from conditional laws. Formally cast into a Bayesian framework, we successfully characterize an exact adjustment factor to account for selections of grouped variables and importantly, provide tractable solutions to bridge the gap between theory and practice. Appealingly amenable to a large class of grouped sparsities and context-relevant targets informed by the associated selections, the efficacy of our methods is evident from the minimal price we pay to correct for selection in comparisons to naive (invalid) inference.

Our methodological advances aligning with a conditional perspective to inference recover uncertainties within group-sparse models across different signal regimes and covariate structures. The performance of these methods serve as an encouraging direction to tackle non-affine geometries in general, seen often with penalties that are disparate in behavior from ℓ_1 sparsity-imposing algorithms. The developments in the work do not preclude proving an asymptotic framework for valid inference after the Group LASSO, when we deviate from Gaussian distributions. Grouped selections form the first step of several exploratory pipelines (for example, in genomic studies) to model responses with better meaning and accuracy. Our solutions for reusing data after a class of grouped selection rules will pave the way to furnish uncertainty estimates in automated models from hierarchical selection pipelines. This leaves room for promising directions of research which we hope to take on as investigations for the future.

Acknowledgements

S.P. and D.K. were supported by NSF-DMS 1951980 and NSF-DMS 1521551 respectively. Data were provided in part by the Human Connectome Project, WU-Minn Consortium (Principal Investigators: David Van Essen and Kamil Ugurbil; 1U54MH091657) funded by the 16 NIH Institutes and Centers that support the NIH Blueprint for Neuroscience Research; and by the McDonnell Center for Systems Neuroscience at Washington University. We thank Dr. Chandra Sripada and his research group (with particular thanks to Saige Rutherford) for providing a processed version of this data.

References

- Sungjin Ahn, Anoop Korattikara, and Max Welling. Bayesian posterior sampling via stochastic gradient fisher scoring. *arXiv preprint arXiv:1206.6380*, 2012.
- Deanna M. Barch, Gregory C. Burgess, Michael P. Harms, Steven E. Petersen, Bradley L. Schlaggar, Maurizio Corbetta, Matthew F. Glasser, Sandra Curtiss, Sachin Dixit, Cindy Feldt, Dan Nolan, Edward Bryant, Tucker Hartley, Owen Footer, James M. Bjork, Russ Poldrack, Steve Smith, Heidi Johansen-Berg, Abraham Z. Snyder, and David C. Van Essen. Function in the human connectome: Task-fMRI and individual differences in behavior. *NeuroImage*, 80:169–189, October 2013. ISSN 1053-8119. doi: 10.1016/j.neuroimage.2013.05.033.
- Yoav Benjamini and Daniel Yekutieli. False discovery rate-adjusted multiple confidence intervals for selected parameters. *Journal of the American Statistical Association*, 100 (469):71–81, 2005.
- Richard Berk, Lawrence Brown, Andreas Buja, Kai Zhang, and Linda Zhao. Valid post-

- selection inference. *The Annals of Statistics*, 41(2):802–837, April 2013. ISSN 0090-5364, 2168-8966. doi: 10.1214/12-AOS1077. URL <http://projecteuclid.org/euclid.aos/1369836961>.
- A De Acosta. Moderate deviations and associated laplace approximations for sums of independent random vectors. *Transactions of the American Mathematical Society*, 329(1):357–375, 1992.
- William Fithian, Dennis Sun, and Jonathan Taylor. Optimal Inference After Model Selection. *arXiv preprint arXiv:1410.2597*, 2014. URL <http://arxiv.org/abs/1410.2597>. arXiv: 1410.2597.
- Jerome Friedman, Trevor Hastie, and Robert Tibshirani. A note on the group lasso and a sparse group lasso. *arXiv preprint arXiv:1001.0736*, 2010.
- Matthew F. Glasser, Stamatios N. Sotiropoulos, J. Anthony Wilson, Timothy S. Coalson, Bruce Fischl, Jesper L. Andersson, Junqian Xu, Saad Jbabdi, Matthew Webster, Jonathan R. Polimeni, David C. Van Essen, and Mark Jenkinson. The minimal preprocessing pipelines for the Human Connectome Project. *NeuroImage*, 80:105–124, October 2013. ISSN 1053-8119. doi: 10.1016/j.neuroimage.2013.04.127.
- Xin Zhou Guo and Xuming He. Inference on selected subgroups in clinical trials. *Journal of the American Statistical Association*, pages 1–19, 2020.
- Tadeusz Inglot and Piotr Majerski. Simple upper and lower bounds for the multivariate laplace approximation. *Journal of Approximation Theory*, 186:1–11, 2014.
- Laurent Jacob, Guillaume Obozinski, and Jean-Philippe Vert. Group Lasso with Overlap and Graph Lasso. In *Proceedings of the 26th Annual International Conference on Ma-*

chine Learning, ICML '09, pages 433–440, New York, NY, USA, 2009a. ACM. ISBN 978-1-60558-516-1. doi: 10.1145/1553374.1553431.

Laurent Jacob, Guillaume Obozinski, and Jean-Philippe Vert. Group lasso with overlap and graph lasso. In *Proceedings of the 26th Annual International Conference on Machine Learning*, ICML '09, pages 433–440, New York, NY, USA, 2009b. ACM. ISBN 978-1-60558-516-1. doi: 10.1145/1553374.1553431. URL <http://doi.acm.org/10.1145/1553374.1553431>.

Todd A Kuffner and G Alastair Young. Principled statistical inference in data science. In *Proceedings of the Statistical Data Science Conference*, 2017.

Jason D. Lee, Dennis L. Sun, Yuekai Sun, and Jonathan E. Taylor. Exact post-selection inference with the lasso. *The Annals of Statistics*, 44(3):907–927, November 2016. URL <http://projecteuclid.org/euclid.aos/1460381681>.

Joshua R Loftus and Jonathan E Taylor. Selective inference in regression models with groups of variables. *arXiv preprint arXiv:1511.01478*, 2015.

Guillaume Obozinski, Laurent Jacob, and Jean-Philippe Vert. Group lasso with overlaps: the latent group lasso approach. *arXiv:1110.0413*, October 2011. URL <http://arxiv.org/abs/1110.0413>.

Snigdha Panigrahi. Carving model-free inference. *arXiv preprint arXiv:1811.03142*, 2018.

Snigdha Panigrahi and Jonathan Taylor. Scalable methods for bayesian selective inference. *Electronic Journal of Statistics*, 12(2):2355–2400, 2018.

Snigdha Panigrahi and Jonathan Taylor. Approximate selective inference via maximum likelihood. *arXiv preprint arXiv:1902.07884*, 2019.

- Snigdha Panigrahi, Jonathan Taylor, and Asaf Weinstein. Integrative methods for post-selection inference under convex constraints. *arXiv preprint arXiv:1605.08824*, 2016. URL <https://arxiv.org/abs/1605.08824>.
- Snigdha Panigrahi, Jelena Markovic, and Jonathan Taylor. An mcmc free approach to post-selective inference. *arXiv preprint arXiv:1703.06154*, 2017.
- Snigdha Panigrahi, Junjie Zhu, and Chiara Sabatti. Selection-adjusted inference: an application to confidence intervals for cis-eQTL effect sizes. *Biostatistics*, 2019. ISSN 1465-4644. doi: 10.1093/biostatistics/kxz024. URL <https://doi.org/10.1093/biostatistics/kxz024>. kxz024.
- Snigdha Panigrahi, Shariq Mohammed, Arvind Rao, and Veerabhadran Baladandayuthapani. Integrative bayesian models using post-selective inference: a case study in radio-genomics. *arXiv preprint arXiv:2004.12012*, 2020.
- Heewon Park, Atushi Niida, Satoru Miyano, and Seiya Imoto. Sparse overlapping group lasso for integrative multi-omics analysis. *Journal of Computational Biology*, 22(2):73–84, 2015.
- KB Petersen, MS Pedersen, et al. The matrix cookbook, vol. 7. *Technical University of Denmark*, 15, 2008.
- Jonathan D. Power, Alexander L. Cohen, Steven M. Nelson, Gagan S. Wig, Kelly Anne Barnes, Jessica A. Church, Alecia C. Vogel, Timothy O. Laumann, Fran M. Miezín, Bradley L. Schlaggar, and Steven E. Petersen. Functional Network Organization of the Human Brain. *Neuron*, 72(4):665–678, November 2011. ISSN 0896-6273. doi: 10.1016/j.neuron.2011.09.006.

- N. Rao, R. Nowak, C. Cox, and T. Rogers. Classification With the Sparse Group Lasso. *IEEE Transactions on Signal Processing*, 64(2):448–463, January 2016. ISSN 1941-0476. doi: 10.1109/TSP.2015.2488586.
- Jesús D. Arroyo Relión, Daniel Kessler, Elizaveta Levina, and Stephan F. Taylor. Network classification with applications to brain connectomics. *The Annals of Applied Statistics*, 13(3):1648–1677, September 2019. ISSN 1932-6157, 1941-7330. doi: 10.1214/19-AOAS1252.
- David Rügamer and Sonja Greven. Inference for l2-boosting. *Statistics and Computing*, 30(2):279–289, 2020.
- Xiaocheng Shang, Zhanxing Zhu, Benedict Leimkuhler, and Amos J Storkey. Covariance-controlled adaptive langevin thermostat for large-scale bayesian sampling. *Advances in Neural Information Processing Systems*, 28:37–45, 2015.
- Yu Shimizu, Junichiro Yoshimoto, Shigeru Toki, Masahiro Takamura, Shinpei Yoshimura, Yasumasa Okamoto, Shigeto Yamawaki, and Kenji Doya. Toward Probabilistic Diagnosis and Understanding of Depression Based on Functional MRI Data Analysis with Logistic Group LASSO. *PLOS ONE*, 10(5):e0123524, May 2015. ISSN 1932-6203. doi: 10.1371/journal.pone.0123524.
- Noah Simon and Robert Tibshirani. Standardization and the group lasso penalty. *Statistica Sinica*, 22(3):983, 2012.
- Noah Simon, Jerome Friedman, Trevor Hastie, and Robert Tibshirani. A sparse-group lasso. *Journal of computational and graphical statistics*, 22(2):231–245, 2013.
- Chandra Sripada, Mike Angstadt, Saige Rutherford, Aman Taxali, and Kerby Shedden. Toward a “treadmill test” for cognition: Improved prediction of general cognitive ability

- from the task activated brain. *Human Brain Mapping*, 41(12):3186–3197, 2020. ISSN 1097-0193. doi: 10.1002/hbm.25007.
- Xiaoying Tian and Jonathan Taylor. Selective inference with a randomized response. *The Annals of Statistics*, 46(2):679–710, 2018.
- Xiaoying Tian, Snigdha Panigrahi, Jelena Markovic, Nan Bi, and Jonathan Taylor. Selective sampling after solving a convex problem. *arXiv preprint arXiv:1609.05609*, 2016.
- Robert Tibshirani. Regression shrinkage and selection via the lasso. *Journal of the Royal Statistical Society: Series B*, 58(1):267–288, 1996. URL <http://onlinelibrary.wiley.com/doi/10.1111/j.1467-9868.2011.00771.x/abstract>.
- Ryan J Tibshirani, Jonathan Taylor, Richard Lockhart, and Robert Tibshirani. Exact post-selection inference for sequential regression procedures. *Journal of the American Statistical Association*, 111(514):600–620, 2016.
- David C. Van Essen, Stephen M. Smith, Deanna M. Barch, Timothy E. J. Behrens, Essa Yacoub, Kamil Ugurbil, and the WU-Minn HCP Consortium. The WU-Minn Human Connectome Project: An overview. *NeuroImage*, 80:62–79, October 2013. ISSN 1053-8119. doi: 10.1016/j.neuroimage.2013.05.041.
- Roderick Wong. *Asymptotic approximations of integrals*. SIAM, 2001.
- 1200 Subjects Data Release Reference Manual*. WU-Minn HCP, 2017. Available at https://www.humanconnectome.org/storage/app/media/documentation/s1200/HCP_S1200_Release_Reference_Manual.pdf.
- Gangcai Xie, Chengliang Dong, Yinfei Kong, Jiang F Zhong, Mingyao Li, and Kai Wang. Group lasso regularized deep learning for cancer prognosis from multi-omics and clinical features. *Genes*, 10(3):240, 2019.

Fan Yang, Rina Foygel Barber, Prateek Jain, and John Lafferty. Selective inference for group-sparse linear models. In *Advances in Neural Information Processing Systems*, pages 2469–2477, 2016.

Daniel Yekutieli. Adjusted bayesian inference for selected parameters. *Journal of the Royal Statistical Society: Series B (Statistical Methodology)*, 74(3):515–541, 2012.

Ming Yuan and Yi Lin. Model selection and estimation in regression with grouped variables. *Journal of the Royal Statistical Society: Series B*, 68(1):49–67, 2005. URL <http://onlinelibrary.wiley.com/doi/10.1111/j.1467-9868.2005.00532.x/abstract>.

SUPPLEMENTARY MATERIAL

A Proofs for technical developments: Section 3

Proof of Theorem 3.1. We write our adjustment factor as follows:

$$\mathbb{P}(\mathcal{A}_E \mid \beta_E) = \int \int L(\beta_E; \hat{\beta}_E) L(\omega \mid \hat{\beta}_E, N_E) \cdot \mathbf{1}_{\mathcal{A}_E}(\hat{\beta}_E, \omega) \, d\omega d\hat{\beta}_E.$$

Next, the change of variables in (11) together with the conditioning upon $\hat{\mathcal{U}} = \mathcal{U}$ and $\hat{\mathcal{Z}} = \mathcal{Z}$ results in the below simplification

$$\mathbb{P}(\mathcal{A}_E \mid \beta_E) = \int \int L(\beta_E; \hat{\beta}_E) L(\hat{\gamma} \mid \mathcal{U}, \mathcal{Z}; \hat{\beta}_E) \cdot \mathbf{1}(\hat{\gamma} > 0) \, d\hat{\gamma} d\hat{\beta}_E. \quad (33)$$

Let $J_{\phi_{\hat{\beta}_E}}(\gamma; \mathcal{U}, \mathcal{Z})$ be the Jacobian associated with the change of variables $\phi_{\hat{\beta}_E}(\cdot)$. Observe, applying the change of variables in (11) gives us:

$$L(\hat{\gamma}, \hat{\mathcal{U}}, \hat{\mathcal{Z}} \mid \hat{\beta}_E) \propto J_{\phi_{\hat{\beta}_E}}(\hat{\gamma}; \hat{\mathcal{U}}, \hat{\mathcal{Z}}) \cdot \exp \left\{ - (A\hat{\beta}_E + B(\hat{\mathcal{U}})\hat{\gamma} + c(\hat{\mathcal{U}}, \hat{\mathcal{Z}}))^{\top} \Omega^{-1} (A\hat{\beta}_E + B(\hat{\mathcal{U}})\hat{\gamma} + c(\hat{\mathcal{U}}, \hat{\mathcal{Z}}))/2 \right\}.$$

Then, we deduce $L(\hat{\gamma} \mid \mathcal{U}, \mathcal{Z}; \hat{\beta}_E)$ is proportional to

$$J_{\phi_{\hat{\beta}_E}}(\hat{\gamma}; \mathcal{U}, \mathcal{Z}) \cdot \exp \left\{ -(\beta_E - \hat{\beta}_E)^\top \Sigma_E^{-1} (\beta_E - \hat{\beta}_E)/2 \right. \\ \left. - (\hat{\gamma} - A^\star \hat{\beta}_E - b^\star)^\top (\Sigma^\star)^{-1} (\hat{\gamma} - A^\star \hat{\beta}_E - b^\star)/2 \right\}.$$

We therefore conclude that (33) is equal to

$$\int \int J_{\phi_{\hat{\beta}_E}}(\hat{\gamma}; \mathcal{U}, \mathcal{Z}) \cdot \exp \left\{ -(\beta_E - \hat{\beta}_E)^\top \Sigma_E^{-1} (\beta_E - \hat{\beta}_E)/2 \right. \\ \left. - (\hat{\gamma} - A^\star \hat{\beta}_E - b^\star)^\top (\Sigma^\star)^{-1} (\hat{\gamma} - A^\star \hat{\beta}_E - b^\star)/2 \right\} \mathbf{1}(\hat{\gamma} > 0) d\hat{\beta}_E d\hat{\gamma},$$

up to a constant.

Left to compute the non trivial Jacobian: $J_{\phi_{\hat{\beta}_E}}(\hat{\gamma}; \mathcal{U}, \mathcal{Z})$, we write the change of variables map in (11) as follows:

$$(\hat{\gamma}, \mathcal{U}, \mathcal{Z}) \xrightarrow{\phi} (\phi_1, \phi_2); \\ \phi_1(\hat{\beta}_E, \hat{\gamma}, \mathcal{U}, \mathcal{Z}) = QU\hat{\gamma} - Q\hat{\beta}_E - ((N_{E,j})_{j \in E}) + ((\lambda_g u_g)_{g \in \mathcal{G}_E}), \quad Q = X_E^\top X_E, \\ \phi_2(\hat{\beta}_E, \hat{\gamma}, \mathcal{U}, \mathcal{Z}) = X_{-E}^\top X_E(U\hat{\gamma} - \hat{\beta}_E) - ((N_{E,j})_{j \in -E}) + ((\lambda_g z_g)_{g \in -\mathcal{G}_E}).$$

Then the derivative matrix can be written as

$$D_{\phi_{\hat{\beta}_E}} = \begin{pmatrix} \frac{\partial \phi_1}{\partial \mathcal{U}} & \frac{\partial \phi_1}{\partial \hat{\gamma}} & \frac{\partial \phi_1}{\partial \mathcal{Z}} \\ \frac{\partial \phi_2}{\partial \mathcal{U}} & \frac{\partial \phi_2}{\partial \hat{\gamma}} & \frac{\partial \phi_2}{\partial \mathcal{Z}} \end{pmatrix},$$

where $\frac{\partial}{\partial \mathcal{U}}(\cdot)$ refers to differentiation with respect to each u_g in the coordinates of its tangent space. Note that the block $\frac{\partial \phi_1}{\partial \mathcal{Z}}$ above the diagonal is zero and $\det \left(\frac{\partial \phi_2}{\partial \mathcal{Z}} \right) \propto 1$. Thus, it follows that

$$J_{\phi_{\hat{\beta}_E}}(\hat{\gamma}; \mathcal{U}, \mathcal{Z}) = \det(D_{\phi_{\hat{\beta}_E}}) \propto \det \left(\begin{pmatrix} \frac{\partial \phi_1}{\partial \mathcal{U}} & \frac{\partial \phi_1}{\partial \hat{\gamma}} \end{pmatrix} \right).$$

First, it is easy to see $\frac{\partial \phi_1}{\partial \hat{\gamma}} = QU$. For computing the other block $\frac{\partial \phi_1}{\partial \mathcal{U}}$, let $u_g \in \mathcal{S}^{|g|-1}$ be associated with the tangent space

$$T_{u_g} \mathcal{S}^{|g|-1} = \{v : v^\top u_g = 0\},$$

the orthogonal complement of $\text{span}\{u_g\}$; \bar{U}_g is a fixed orthonormal basis for this tangent space. For a vector of coordinates $y_g \in \mathbb{R}^{|g|-1}$ and a general function h ,

$$\frac{\partial h(u_g)}{\partial u_g} := \frac{\partial h(u_g + \bar{U}_g y_g)}{\partial y_g}.$$

Writing this more compactly with a stacked vector $y = (y_1, \dots, y_{|\mathcal{G}_E|})^\top$, it follows that for fixed g ,

$$\begin{aligned} \frac{\partial \phi_1}{\partial u_g} &= \frac{\partial}{\partial y_g} \{Q(U + \bar{U}y)\hat{\gamma} + ((\lambda_g(u_g + \bar{U}_g y_g))_{g \in E})\} \\ &= Q \begin{pmatrix} 0 & \dots & (\hat{\gamma}_g \bar{U}_g)^\top & \dots & 0 \end{pmatrix}^\top + \begin{pmatrix} 0 & \dots & (\lambda_g \bar{U}_g)^\top & \dots & 0 \end{pmatrix}^\top, \end{aligned}$$

and combining these column-wise we obtain the full derivative matrix

$$\begin{aligned} \frac{\partial \phi_1}{\partial \mathcal{U}} &= \begin{pmatrix} \frac{\partial \phi_1}{\partial u_1} & \dots & \frac{\partial \phi_1}{\partial u_{|\mathcal{G}_E|}} \end{pmatrix} = Q \cdot \text{diag}((\hat{\gamma}_g \bar{U}_g)_{g \in E}) + \text{diag}((\lambda_g \bar{U}_g)_{g \in E}) \\ &= Q \bar{\Gamma} \bar{U} + \Lambda \bar{U}; \quad \text{where } \bar{\Gamma} = \text{diag}((\hat{\gamma}_g I_{|g|})_{g \in \mathcal{G}_E}), \\ &= (Q \bar{\Gamma} + \Lambda) \bar{U}. \end{aligned}$$

This gives us

$$\det(D_{\phi_{\hat{\beta}_E}}) \propto \det \begin{pmatrix} (Q \bar{\Gamma} + \Lambda) \bar{U} & QU \end{pmatrix}. \quad (34)$$

Simplifying this expression further, we multiply by the constant (with respect to $\hat{\gamma}$)

$$\det \left(\begin{pmatrix} \bar{U}^\top \\ U^\top \end{pmatrix} Q^{-1} \right),$$

which finally leads to

$$\begin{aligned} \det(D_{\phi_{\hat{\beta}_E}}) &\propto \det \left(\begin{pmatrix} \bar{U}^\top \\ U^\top \end{pmatrix} (\bar{\Gamma} \bar{U} + Q^{-1} \Lambda \bar{U} \quad U) \right) \\ &= \det \left(\begin{pmatrix} \Gamma + \bar{U}^\top Q^{-1} \Lambda \bar{U} & 0 \\ \dots & I_{|E|} \end{pmatrix} \right) \\ &= \det(\Gamma + \bar{U}^\top Q^{-1} \Lambda \bar{U}), \end{aligned}$$

where the second to last equality follows since $\bar{U}^\top \bar{\Gamma} \bar{U} = \Gamma$ by block orthogonality, and the final equality follows by block triangularity. This proves our claim in the Theorem. \square

Proof of Theorem 3.2. To derive the expression in (15), we note that optimizing over $\tilde{\beta}_E$ in the problem:

$$\text{minimize}_{\tilde{\beta}_E, \tilde{\gamma}} \left\{ \frac{1}{2}(\tilde{\beta}_E - \beta_E)^\top \Sigma_E^{-1}(\tilde{\beta}_E - \beta_E) + \frac{1}{2}(\tilde{\gamma} - A^* \tilde{\beta}_E - b^*)^\top (\Sigma^*)^{-1}(\tilde{\gamma} - A^* \tilde{\beta}_E - b^*) + \text{Barr}(\tilde{\gamma}) \right\}$$

gives us

$$\text{minimize}_\gamma \frac{1}{2}(\gamma - \bar{P}\beta_E - \bar{q})^\top (\bar{\Sigma})^{-1}(\gamma - \bar{P}\beta_E - \bar{q}) + \text{Barr}(\gamma).$$

Plugging in the value of this optimization into (13), the logarithm of the surrogate posterior is given by the expression

$$\begin{aligned} \log \pi(\beta_E) + \log L(\beta_E; \hat{\beta}_E) + \frac{1}{2}(\gamma^* - \bar{P}\beta_E - \bar{q})^\top (\bar{\Sigma})^{-1}(\gamma^* - \bar{P}\beta_E - \bar{q}) + \text{Barr}(\gamma^*) \\ - \log J_\phi(\gamma^*; \mathcal{U}). \end{aligned}$$

To compute the gradient of the (log) surrogate posterior, define $\zeta^*(\cdot)$ to be the convex conjugate for the function

$$\zeta(\gamma) = \frac{1}{2}\gamma^\top (\bar{\Sigma})^{-1}\gamma + \text{Barr}(\gamma).$$

This allows us to write (15) in the below form

$$\begin{aligned} \log \pi(\beta_E) - \frac{1}{2}(\hat{\beta}_E - \beta_E)^\top \Sigma_E^{-1}(\hat{\beta}_E - \beta_E) + \frac{1}{2}(\bar{P}\beta_E + \bar{q})^\top (\bar{\Sigma})^{-1}(\bar{P}\beta_E + \bar{q}) \\ - \zeta^*((\bar{\Sigma})^{-1}(\bar{P}\beta_E + \bar{q})) - \log J_\phi(\gamma^*; \mathcal{U}). \end{aligned} \tag{35}$$

Denoting $L(\beta_E) = (\bar{\Sigma})^{-1}(\bar{P}\beta_E + \bar{q})$ and taking the derivative of (35) with respect to β_E

gives us:

$$\begin{aligned}
& \nabla \log \pi(\beta_E) + \Sigma_E^{-1}(\hat{\beta}_E - \beta_E) + \bar{P}^\top(\bar{\Sigma})^{-1}(\bar{P}\beta_E + \bar{q}) \\
& - \bar{P}^\top(\bar{\Sigma})^{-1} \nabla_{L(\beta_E)} \zeta^*((\bar{\Sigma})^{-1}(\bar{P}\beta_E + \bar{q})) - \bar{P}^\top(\bar{\Sigma})^{-1} \nabla_{L(\beta_E)} \gamma^*((\bar{\Sigma})^{-1}(\bar{P}\beta_E + \bar{q})) \nabla_{\gamma^*} \log J_\phi(\gamma^*; \mathcal{U}) \\
& = \nabla \log \pi(\beta_E) + \Sigma_E^{-1}(\hat{\beta}_E - \beta_E) + \bar{P}^\top(\bar{\Sigma})^{-1}(\bar{P}\beta_E + \bar{q}) \\
& - \bar{P}^\top(\bar{\Sigma})^{-1}(\nabla_{L(\beta_E)} \zeta)^{-1}(L(\beta_E)) - \bar{P}^\top(\bar{\Sigma})^{-1} \nabla_{L(\beta_E)} \gamma^*(L(\beta_E)) \nabla_{\gamma^*} \log J_\phi(\gamma^*; \mathcal{U}) \\
& = \nabla \log \pi(\beta_E) + \Sigma_E^{-1}(\hat{\beta}_E - \beta_E) + \bar{P}^\top(\bar{\Sigma})^{-1}(\bar{P}\beta_E + \bar{q}) \\
& - \bar{P}^\top(\bar{\Sigma})^{-1} \gamma^*(L(\beta_E)) - \bar{P}^\top(\bar{\Sigma})^{-1} \nabla_{L(\beta_E)} \gamma^*(L(\beta_E)) \nabla_{\gamma^*} \log J_\phi(\gamma^*; \mathcal{U}).
\end{aligned}$$

Note, we use the fact: $\nabla \zeta^*(\cdot) = (\nabla \zeta)^{-1}(\cdot)$ in the second display and the third display follows by observing: $(\nabla \zeta)^{-1}(L(\beta_E)) = \gamma^*(L(\beta_E))$ where

$$\gamma^* = \operatorname{argmax}_{\gamma} \gamma^\top L(\beta_E) - \zeta(\gamma),$$

further equal to the optimizer defined in

$$\operatorname{argmin}_{\gamma} \frac{1}{2}(\gamma - \bar{P}\beta_E - \bar{q})^\top(\bar{\Sigma})^{-1}(\gamma - \bar{P}\beta_E - \bar{q}) + \text{Barr}(\gamma).$$

Computing the two pieces in the gradient $\nabla_{L(\beta_E)} \gamma^*(L(\beta_E))$ and $\nabla_{\gamma^*} \log J_\phi(\gamma^*; \mathcal{U})$, we first have

$$\nabla \gamma^*(\cdot) = \nabla^2 \zeta^*(\cdot) = [\nabla^2 \zeta(\gamma^*(\cdot))]^{-1}.$$

Since $\nabla^2 \zeta(\gamma) = \bar{\Sigma}^{-1} + \nabla^2 \text{Barr}(\gamma)$, we have

$$\nabla_{L(\beta_E)} \gamma^*(L(\beta_E)) = (\bar{\Sigma}^{-1} + \nabla^2 \text{Barr}(\gamma^*(L(\beta_E))))^{-1}.$$

As for $\nabla \log J_\phi(\gamma^*; \mathcal{U})$, recall from Theorem 3.1

$$J_\phi(\gamma; \mathcal{U}) = \det(\Gamma + \bar{U}^\top(X_E^\top X_E)^{-1} \Lambda \bar{U}).$$

We have the following matrix derivative identities for a square matrix X [Petersen et al., 2008]:

$$\frac{\partial \log \det(X)}{\partial X_{ij}} = (X^{-1})_{ji}, \frac{\partial (X^{-1})_{kl}}{\partial X_{ij}} = -(X^{-1})_{ki}(X^{-1})_{jl}. \quad (36)$$

Using the chain rule:

$$\gamma \xrightarrow{J_1} (\Gamma + \bar{U}^\top (X_E^\top X_E)^{-1} \Lambda \bar{U}) \xrightarrow{J_2} \log \det(\Gamma + \bar{U}^\top (X_E^\top X_E)^{-1} \Lambda \bar{U}),$$

we partition the indices into $\{M_g\}_{g \in E}$ such that M_g is the set of $|g| - 1$ indices along the diagonal of Γ corresponding to group g . Then

$$\left[\frac{\partial J_1}{\partial \gamma_g} \right]_{ij} = \begin{cases} 1, & i = j, i \in M_g, \\ 0, & \text{otherwise.} \end{cases}$$

By (36), the partial derivatives of J_2 are the entries of $(\Gamma + \bar{U}^\top (X_E^\top X_E)^{-1} \Lambda \bar{U})^{-1}$. Putting these together,

$$\frac{\partial \log J_\phi(\cdot; \mathcal{U})}{\partial \gamma_g} = \sum_{i \in M_g} [(\Gamma + \bar{U}^\top (X_E^\top X_E)^{-1} \Lambda \bar{U})^{-1}]_{ii},$$

which gives us the expression for $\nabla_{\gamma^*} \log J_\phi(\gamma^*; \mathcal{U})$. \square

B Proofs for large sample theory: Section 5

We provide in this section the proofs of the large sample claims for our selection-informed posterior in Section 5. Supporting results for this theory, Lemma 1 and 2, are included in Section C.

Proof of Proposition 5.1. First, observe that we write our probability of selection as follows:

$$(b_n)^{-2} \log \mathbb{P} (0 < \sqrt{n} \gamma_n < b_n \bar{Q} \cdot \mathbf{1}_{|E|} + \bar{q}) = (b_n)^{-2} \log \mathbb{E} \left[\exp(\log J_\phi(\sqrt{n} \bar{Z}_n + b_n \bar{P} \bar{\beta}_E + \bar{q}; \mathcal{U})) \right. \\ \left. \times 1(-b_n \bar{P} \bar{\beta}_E - \bar{q} < \sqrt{n} \bar{Z}_n < b_n \bar{Q} \cdot \mathbf{1}_{|E|} - b_n \bar{P} \bar{\beta}_E) \right],$$

(up to an additive constant), where $\sqrt{n} \bar{Z}_n$ is a centered gaussian random variable with covariance $\bar{\Sigma}$. Define $\mathcal{C}_0 = \{z : -\bar{P} \bar{\beta}_E < z < \bar{Q} \cdot \mathbf{1}_{|E|} - \bar{P} \bar{\beta}_E\}$. Using assumption (30), we

deduce

$$\begin{aligned}
& \limsup_{n \rightarrow \infty} (b_n)^{-2} \log \mathbb{P} \left(0 < \sqrt{n} \gamma_n < b_n \bar{Q} \cdot \mathbf{1}_{|E|} + \bar{q} \right) \\
&= \limsup_{n \rightarrow \infty} (b_n)^{-2} \log \mathbb{E} \left[\exp(\log J_\phi(\sqrt{n} \bar{Z}_n + b_n \bar{P} \bar{\beta}_E + \bar{q}; \mathcal{U})) \cdot \mathbf{1}_{\mathcal{C}_0}(\sqrt{n} \bar{Z}_n / b_n) \right] \\
&\leq \lim_{n \rightarrow \infty} \sup_{z \in \mathcal{C}_0} (b_n)^{-2} |\log J_\phi(b_n z + b_n \bar{P} \bar{\beta}_E + \bar{q}; \mathcal{U})| + \lim_{n \rightarrow \infty} (b_n)^{-2} \log \mathbb{P} \left(\sqrt{n} \bar{Z}_n / b_n \in \mathcal{C}_0 \right) \\
&= \lim_{n \rightarrow \infty} (b_n)^{-2} \log \mathbb{P} \left(-\bar{P} \bar{\beta}_E < \sqrt{n} \bar{Z}_n / b_n < \bar{Q} \cdot \mathbf{1}_{|E|} - \bar{P} \bar{\beta}_E \right).
\end{aligned}$$

To justify that the limit of the term involving the Jacobian vanishes, note that for all $z \in \mathcal{C}_0$, we have

$$\bar{q} < b_n z + b_n \bar{P} \bar{\beta}_E + \bar{q} < b_n \bar{Q} \mathbf{1}_{|E|} + \bar{q}.$$

Thus, $J_\phi(b_n z + b_n \bar{P} \bar{\beta}_E + \bar{q}; \mathcal{U})$ is the determinant of a matrix with entries uniformly bounded by $2b_n \bar{Q} > 0$ for sufficiently large n . Then

$$\sup_{z \in \mathcal{C}_0} |J_\phi(b_n z + b_n \bar{P} \bar{\beta}_E + \bar{q}; \mathcal{U})| \leq |E|! (2b_n \bar{Q})^{|E|}.$$

The Jacobian is also bounded away from zero, thus it follows that

$$\sup_{z \in \mathcal{C}_0} (b_n)^{-2} |\log J_\phi(b_n z + b_n \bar{P} \bar{\beta}_E + \bar{q}; \mathcal{U})| \leq (b_n)^{-2} \log \left(|E|! (2b_n \bar{Q})^{|E|} \right)$$

which goes to 0 as $n \rightarrow \infty$. Using an argument along the same line,

$$\begin{aligned}
& \liminf_{n \rightarrow \infty} (b_n)^{-2} \log \mathbb{P} \left(0 < \sqrt{n} \gamma_n < b_n \bar{Q} \cdot \mathbf{1}_{|E|} + \bar{q} \right) \\
&\geq - \lim_{n \rightarrow \infty} \sup_{z \in \mathcal{C}_0} (b_n)^{-2} |\log J_\phi(b_n z + b_n \bar{P} \bar{\beta}_E + \bar{q}; \mathcal{U})| + \lim_{n \rightarrow \infty} (b_n)^{-2} \log \mathbb{P} \left(\sqrt{n} \bar{Z}_n / b_n \in \mathcal{C}_0 \right).
\end{aligned}$$

From the above limits, we have

$$\lim_{n \rightarrow \infty} (b_n)^{-2} \left(\log \mathbb{P} \left(0 < \sqrt{n} \gamma_n < b_n \bar{Q} \cdot \mathbf{1}_{|E|} + \bar{q} \right) - \log \mathbb{P} \left(\sqrt{n} \bar{Z}_n / b_n \in \mathcal{C}_0 \right) \right) = 0.$$

Using a moderate (large)-deviation type result [De Acosta, 1992] for the limiting value of the probability in the second term, we have

$$\lim_{n \rightarrow \infty} (b_n)^{-2} \log \mathbb{P} \left(0 < \sqrt{n} \gamma_n < b_n \bar{Q} \cdot \mathbf{1}_{|E|} + \bar{q} \right) + \inf_{z \in \mathcal{C}_0} z^\top \bar{\Sigma}^{-1} z / 2 = 0.$$

Lastly, we let $z + \bar{P}\bar{\beta}_E + (b_n)^{-1}\bar{q} = \bar{\gamma}$. Using the observation that the optimization $\inf_{z \in \mathcal{C}_0} z^\top \bar{\Sigma}^{-1} z$ has a unique minimum, and relying on the convexity of the objectives in the sequence of optimization problems defined below

$$\inf_{\bar{\gamma} < \bar{Q} \cdot \mathbf{1}_{|E|}} \left\{ \frac{1}{2} (\bar{\gamma} - \bar{P}\bar{\beta}_E - (b_n)^{-1}\bar{q})^\top \bar{\Sigma}^{-1} (\bar{\gamma} - \bar{P}\bar{\beta}_E - (b_n)^{-1}\bar{q}) + (b_n)^{-2} \text{Barr}(b_n \bar{\gamma}) \right\},$$

our claim in the Proposition is complete. \square

Notice, we work with the below approximation for the adjustment factor in Theorem 3.1:

$$\exp \left(-\frac{b_n^2}{2} (\bar{\gamma}_n^* - \bar{P}\bar{\beta}_E - (b_n)^{-1}\bar{q})^\top \bar{\Sigma}^{-1} (\bar{\gamma}_n^* - \bar{P}\bar{\beta}_E - (b_n)^{-1}\bar{q}) - \text{Barr}(b_n \bar{\gamma}_n^*) + \log J_\phi(b_n \bar{\gamma}_n^*; \mathcal{U}) \right),$$

motivated by Proposition 5.1 where

$$\bar{\gamma}_n^* = \text{argmin} \frac{1}{2} (\bar{\gamma} - \bar{P}\bar{\beta}_E - (b_n)^{-1}\bar{q})^\top \bar{\Sigma}^{-1} (\bar{\gamma} - \bar{P}\bar{\beta}_E - (b_n)^{-1}\bar{q}) + (b_n)^{-2} \text{Barr}(b_n \bar{\gamma}). \quad (37)$$

Proof of Proposition 5.2. Set $\sqrt{n}z_n = b_n \bar{z}$ and let $\bar{\gamma}_n^*$ be the optimizer defined in (37). Then, the surrogate selection-informed (log) likelihood assumes the below form

$$\ell_{n,S}(z_n; \hat{\beta}_{n,E} \mid N_{n,E}) = (\sqrt{n} \hat{\beta}_{n,E})^\top \Sigma_E^{-1} b_n \bar{z} - b_n^2 C_n(\bar{z}). \quad (38)$$

In the above representation, $C_n(\bar{z})$ equals

$$\begin{aligned} & (\bar{\gamma}_n^*)^\top (\bar{\Sigma})^{-1} (\bar{P}\bar{z} + (b_n)^{-1}\bar{q}) - \frac{1}{2} (\bar{\gamma}_n^*)^\top (\bar{\Sigma})^{-1} \bar{\gamma}_n^* - (b_n)^{-2} \text{Barr}(b_n \bar{\gamma}_n^*) \\ & + (b_n)^{-2} \log J_\phi(b_n \bar{\gamma}_n^*; \mathcal{U}) + \frac{1}{2} \bar{z}^\top \Sigma_E^{-1} (\Sigma_E^{-1} + A^{*\top} (\Sigma^*)^{-1} A^*)^{-1} \Sigma_E^{-1} \bar{z} + \bar{z}^\top \bar{P}^\top \bar{\Sigma}^{-1} \bar{q} / b_n, \end{aligned}$$

which we derive after plugging in the associated (log) approximation.

Next, we define the below constants: C_1 is the largest eigen value of Σ_E^{-1} and C_0 is the smallest eigen value of $\Sigma_E^{-1} (\Sigma_E^{-1} + A^{*\top} (\Sigma^*)^{-1} A^*)^{-1} \Sigma_E^{-1}$. Consistent with our parameterization, we denote $b_n \bar{\beta}_E^{\max} = \sqrt{n} \hat{\beta}_{n,E}^{\max}$. It follows then from a Taylor series expansion of

$C_n(\bar{z})$ around $\bar{\beta}_E^{\max}$ that the difference of log-likelihoods

$$\ell_{n,S}(z_n; \hat{\beta}_{n,E} \mid N_{n,E}) - \ell_{n,S}(\hat{\beta}_{n,E}^{\max}; \hat{\beta}_{n,E} \mid N_{n,E})$$

equals

$$\begin{aligned} & \sqrt{n}(\hat{\beta}_{n,E})^\top \Sigma_E^{-1} b_n(\bar{z} - \bar{\beta}_E^{\max}) - (b_n)^2 \{C_n(\bar{z}) - C_n(\bar{\beta}_E^{\max})\} \\ &= b_n(\bar{z} - \bar{\beta}_E^{\max})^\top \Sigma_E^{-1} \sqrt{n} \hat{\beta}_{n,E} - (b_n)^2 (\bar{z} - \bar{\beta}_E^{\max})^\top \nabla C_n(\bar{\beta}_E^{\max}) \\ & \quad - (b_n)^2 (\bar{z} - \bar{\beta}_E^{\max})^\top \nabla^2 C_n(R(\bar{\beta}_E^{\max}; \bar{z})) (\bar{z} - \bar{\beta}_E^{\max})/2 \\ &= -n(z_n - \hat{\beta}_{n,E}^{\max})^\top \nabla^2 C_n(R(\bar{\beta}_E^{\max}; \bar{z})) (z_n - \hat{\beta}_{n,E}^{\max})/2. \end{aligned}$$

By Lemma 2, there exists $N \in \mathbb{N}$ such that the contribution of the Jacobian term to the Hessian ($\nabla^2 C_n(\cdot)$),

$$\sup_{\bar{z} \in \mathcal{C}} \|\nabla_{\bar{z}}^2(b_n)^{-2} \log J_\phi(b_n \bar{\gamma}_n^*(\bar{z}); \mathcal{U})\|_{\text{op}}$$

is uniformly bounded in operator norm by ϵ_0 for all $n \geq N$. Finally, noting

$$(\bar{\gamma}_n^*)^\top (\bar{\Sigma})^{-1} (\bar{P}\bar{z} + (b_n)^{-1}\bar{q}) - \frac{1}{2}(\bar{\gamma}_n^*)^\top (\bar{\Sigma})^{-1} \bar{\gamma}_n^* - (b_n)^{-2} \text{Barr}(b_n \bar{\gamma}_n^*)$$

is a convex conjugate of the function $(\bar{\gamma})^\top (\bar{\Sigma})^{-1} \bar{\gamma}/2 + (b_n)^{-2} \text{Barr}(b_n \bar{\gamma})$ evaluated at $\bar{\Sigma}^{-1}(\bar{P}\bar{z} + (b_n)^{-1}\bar{q})$, we conclude

$$(C_0 - \epsilon_0) \cdot I \preceq \nabla^2 C_n(\bar{z}) \preceq (C_1 + \epsilon_0) \cdot I$$

for all $\bar{z} \in \mathcal{C}$. This directly leads to our claim in the Proposition. \square

Proof of Theorem 5.1. Fix $0 < a < 1$ such that

$$4a^2 \cdot (C_1 + C_0/2) - (1-a)^2 \cdot C_0/2 < 0,$$

where C_0 and C_1 are defined in Proposition 5.2. This follows by noting that the quadratic expression on the left-hand side has a root between $(0, 1)$. Denoting $\mathcal{C} \cap \mathcal{B}^c(\beta_{n,E}, \delta_n) = \mathcal{B}'^c(\beta_{n,E}, \delta_n)$, we observe that there exists N such that for all $n \geq N$ such that

$$\begin{aligned}
& \mathbb{P}_{n,S} \left(\Pi_{n,S} \left(\mathcal{B}^c(\beta_{n,E}, \delta_n) \mid \widehat{\beta}_{n,E}; N_{n,E} \right) \leq \epsilon \right) \\
&= \mathbb{P}_{n,S} \left(\int_{\mathcal{B}'^c(\beta_{n,E}, \delta_n)} \pi(z_n) \cdot \exp(\ell_{n,S}(z_n; \widehat{\beta}_{n,E} | N_{n,E})) dz_n \leq \epsilon \int \pi(z_n) \cdot \exp(\ell_{n,S}(z_n; \widehat{\beta}_{n,E} | N_{n,E})) dz_n \right) \\
&\geq \mathbb{P}_{n,S} \left(\int_{\mathcal{B}'^c(\beta_{n,E}, \delta_n)} \pi(z_n) \cdot \exp(\ell_{n,S}(z_n; \widehat{\beta}_{n,E} | N_{n,E}) - \ell_{n,S}(\widehat{\beta}_{n,E}^{\max}; \widehat{\beta}_{n,E} | N_{n,E})) dz_n \right. \\
&\quad \left. \leq \epsilon \int_{\mathcal{B}(\beta_{n,E}, a\delta_n)} \pi(z_n) \cdot \exp(\ell_{n,S}(z_n; \widehat{\beta}_{n,E} | N_{n,E}) - \ell_{n,S}(\widehat{\beta}_{n,E}^{\max}; \widehat{\beta}_{n,E} | N_{n,E})) dz_n \right) \\
&\geq \mathbb{P}_{n,S} \left(\int_{\mathcal{B}'^c(\beta_{n,E}, \delta_n)} \pi(z_n) \cdot \exp(-nC_0 \cdot \|\widehat{\beta}_{n,E}^{\max} - z_n\|^2/4) dz_n \right. \\
&\quad \left. \leq \epsilon \int_{\mathcal{B}(\beta_{n,E}, a\delta_n)} \pi(z_n) \cdot \exp(-n(C_1 + C_0/2) \cdot \|\widehat{\beta}_{n,E}^{\max} - z_n\|^2/2) dz_n \right).
\end{aligned}$$

The ultimate display follows by using the bounds in Proposition 5.2 where we set $\epsilon_0 = C_0/2$. This yields us the following lower bound for $\mathbb{P}_{n,S} \left(\Pi_{n,S} \left(\mathcal{B}^c(\beta_{n,E}, \delta_n) \mid \widehat{\beta}_{n,E}; N_{n,E} \right) \leq \epsilon \right)$:

$$\begin{aligned}
& \mathbb{P}_{n,S} \left(\int_{\mathcal{B}'^c(\beta_{n,E}, \delta_n)} \pi(z_n) \cdot \exp(-nC_0 \cdot \|\widehat{\beta}_{n,E}^{\max} - z_n\|^2/4) dz_n \right. \\
&\quad \leq \epsilon \int_{\mathcal{B}(\beta_{n,E}, a\delta_n)} \pi(z_n) \cdot \exp(-n(C_1 + C_0/2) \cdot \|\widehat{\beta}_{n,E}^{\max} - z_n\|^2/2) dz_n, \\
&\quad \|\widehat{\beta}_{n,E}^{\max} - z_n\| \geq (1-a)\delta_n \text{ for all } z_n \in \mathcal{B}'^c(\beta_{n,E}, \delta_n), \\
&\quad \left. \|\widehat{\beta}_{n,E}^{\max} - z_n\| \leq 2a\delta_n \text{ for all } z_n \in \mathcal{B}(\beta_{n,E}, a\delta_n) \right)
\end{aligned}$$

$$\begin{aligned}
&\geq \mathbb{P}_{n,S} \left(\exp(-C_0 \cdot (1-a)^2 n \delta_n^2 / 4) \leq \epsilon \cdot \Pi(\mathcal{B}(\beta_{n,E}, a\delta_n)) \exp(-(C_1 + C_0/2) \cdot 4a^2 \delta_n^2 / 2) \right. \\
&\quad \left. \begin{aligned} &\|\hat{\beta}_{n,E}^{\max} - z_n\| \geq (1-a)\delta_n \text{ for all } z_n \in \mathcal{B}'^c(\beta_{n,E}, \delta_n), \\ &\|\hat{\beta}_{n,E}^{\max} - z_n\| \leq 2a\delta_n \text{ for all } z_n \in \mathcal{B}(\beta_{n,E}, a\delta_n) \end{aligned} \right) \\
&\geq \mathbb{P}_{n,S}(\|\hat{\beta}_{n,E}^{\max} - \beta_{n,E}\| \leq a\delta_n).
\end{aligned}$$

The argument in the last display follows from our assumptions on the prior for sufficiently large n , coupled with the choice of $a \in (0, 1)$. We complete our proof by showing

$$\lim_{n \rightarrow \infty} \mathbb{P}_{n,S}(\|\hat{\beta}_{n,E}^{\max} - \beta_{n,E}\| > a\delta_n) = 0.$$

To this end, we note that the MLE estimating equation is given by:

$$\sqrt{n} \Sigma_E^{-1} \hat{\beta}_{n,E} = b_n \nabla C_n(\bar{\beta}_E^{\max})$$

from the surrogate selection-informed (log) likelihood in (38) (Proposition 5.2) under our parameterization. Further, observing that $C_n(\cdot)$ is strongly convex for sufficiently large n , we have

$$(L)^{-2} \|\sqrt{n} \Sigma_E^{-1} \hat{\beta}_{n,E} - b_n \nabla C_n(\bar{\beta}_E)\|^2 \geq \|\sqrt{n} \hat{\beta}_{n,E}^{\max} - \sqrt{n} \beta_{n,E}\|^2;$$

$L = C_0/2$. Denoting the exact counterpart of $C_n(\cdot)$ (obtained upon using the exact probability of selection) by $\bar{C}_n(\cdot)$, we conclude

$$\begin{aligned}
\mathbb{P}_{n,S}((b_n)^{-1} \sqrt{n} \|\hat{\beta}_{n,E}^{\max} - \beta_{n,E}\| > a\delta) &\leq (b_n a \delta L)^{-2} \cdot \mathbb{E}_{n,S}(\|\sqrt{n} \Sigma_E^{-1} \hat{\beta}_{n,E} - b_n \nabla C_n(\bar{\beta}_E)\|^2) \\
&\leq (b_n a \delta L)^{-2} \cdot \mathbb{E}_{n,S}(\|\sqrt{n} \Sigma_E^{-1} \hat{\beta}_{n,E} - b_n \nabla \bar{C}_n(\bar{\beta}_E)\|^2) \\
&\quad + (a \delta L)^{-2} \cdot \|\nabla C_n(\bar{\beta}_E) - \nabla \bar{C}_n(\bar{\beta}_E)\|^2.
\end{aligned}$$

The first term in the final display clearly converges to 0 as $n \rightarrow \infty$. The second term converges to 0, using the result in Proposition 5.1 combined with the convexity and smoothness of the sequence $C_n(\cdot)$ for large enough n . \square

C Supporting theory: Section 5

Below, we prove a result on the asymptotic orders of the gradient and Hessian of the (log) Jacobian; this in turn allows us to bound the contribution of the Jacobian term in the Hessian of the (log) likelihood in Proposition 5.2.

Lemma 1. *For $\eta > 0$, denote*

$$\mathcal{K}_\eta = \{x \in \mathbb{R}^{|E|} : \min_j x_j > \eta\}. \quad (39)$$

We have then the following uniform bounds on the derivatives of the (log) Jacobian:

$$\begin{aligned} \sup_{x \in \mathcal{K}_\eta} \|\nabla_\gamma \log J_\phi(\gamma; \mathcal{U})|_{b_n x}\|_\infty &= O(b_n^{-1}), \\ \sup_{x \in \mathcal{K}_\eta} \|\nabla_\gamma^2 \log J_\phi(\gamma; \mathcal{U})|_{b_n x}\|_{op} &= O(b_n^{-2}). \end{aligned}$$

Proof. We begin by deriving an expression for the Hessian $\nabla_\gamma^2 \log J_\phi(\gamma; \mathcal{U})$. Recall from Theorem 3.2, for $g = 1, \dots, |E|$,

$$\frac{\partial}{\partial \gamma_g} \log J_\phi(\gamma; \mathcal{U}) = \sum_{i \in M_g} [(\Gamma + C)^{-1}]_{ii}, \quad (40)$$

where for simplicity we denote $C = \bar{U}^\top (X_E^\top X_E)^{-1} \Lambda \bar{U}$, $\Gamma = \text{diag}((\gamma_g I_{|g|-1})_{g \in \mathcal{G}_E})$, and M_g denotes the set of indices along the diagonal of Γ corresponding to group g . Using matrix derivative identities similar to those applied in the proof of Theorem 3.2, we derive for $g, h = 1, \dots, |E|$,

$$\frac{\partial^2}{\partial \gamma_g \partial \gamma_h} \log J_\phi(\gamma; \mathcal{U}) = - \sum_{i \in M_g} \sum_{j \in M_h} [(\Gamma + C)^{-1}]_{ij} \cdot [\{(\Gamma + C)^{-1}\}^\top]_{ij} \quad (41)$$

Both our claims rely on a uniform bound on the entries of $(\Gamma + C)^{-1}$. Let the operators s_{\max} , λ_{\max} and λ_{\min} denote the largest singular value, largest eigenvalue, and smallest

eigenvalue of a matrix respectively. Fix $x \in \mathcal{K}_\eta$; let $\Gamma(b_n x) = \text{diag}((b_n x_g I_{|g|-1})_{g \in \mathcal{G}_E})$. Denote its dimension by $q = \sum_{g \in E} (|g| - 1)$. Then

$$\begin{aligned} \max_{1 \leq i, j \leq q} |[(\Gamma(b_n x) + C)^{-1}]_{ij}| &\leq s_{\max}((\Gamma(b_n x) + C)^{-1}) \\ &= \lambda_{\max}^{1/2}((\Gamma(b_n x) + C)^{-1} [(\Gamma(b_n x) + C)^{-1}]^\top) \\ &= \lambda_{\min}^{-1/2}((\Gamma(b_n x) + C)^\top (\Gamma(b_n x) + C)). \end{aligned}$$

Now note the following:

$$\begin{aligned} \lambda_{\min}((\Gamma(b_n x) + C)^\top (\Gamma(b_n x) + C)) &= \inf_{\|v\|_2=1} v^\top ((\Gamma(b_n x) + C)^\top (\Gamma(b_n x) + C)) v \\ &\geq b_n^2 \min_{1 \leq j \leq |E|} x_j^2 + \lambda_{\min}(C^\top C) \\ &\geq (b_n \eta)^2. \end{aligned}$$

Combining the previous two displays uniformly over \mathcal{K}_η , we have that

$$\sup_{x \in \mathcal{K}_\eta} \left(\max_{1 \leq i, j \leq q} |[(\Gamma(b_n x) + C)^{-1}]_{ij}| \right) \leq \frac{1}{b_n \eta} = O(b_n^{-1}). \quad (42)$$

By (40), each entry of the gradient is the sum of up to $p - 1$ entries of $(\Gamma(b_n x) + C)^{-1}$, and by (41), each entry of the Hessian is a sum of up to p^2 products of entries of the same matrix. Lastly, a bound on the ℓ_∞ norm of the gradient follows directly from this element-wise bound. Further, a bound for the operator norm of the Hessian follows after noting that for an $r \times r$ square matrix M , $\|M\|_2 \leq r \max_{ij} |M_{ij}|$. \square

With the previous result in hand, we prove the next Lemma used in Proposition 5.2.

Lemma 2. *Under the assumptions of Proposition 5.2, we have*

$$\lim_{n \rightarrow \infty} \left\{ \sup_{\bar{z} \in \mathcal{C}} \|\nabla_{\bar{z}}^2(b_n)^{-2} \log J_\phi(b_n \bar{\gamma}_n^*(\bar{z}); \mathcal{U})\|_{op} \right\} = 0.$$

Proof. To proceed with the proof, we derive an expression for the Hessian of the (log) Jacobian. Recall, $\bar{\gamma}_n^*(\bar{z})$ is the optimizer of the convex conjugate of the function

$$(\bar{\gamma})^\top (\bar{\Sigma})^{-1} \bar{\gamma} / 2 + (b_n)^{-2} \text{Barr}(b_n \bar{\gamma})$$

evaluated at $\bar{\Sigma}^{-1}(\bar{P}\bar{z} + (b_n)^{-1}\bar{q})$. By properties of the convex conjugate function and the chain rule,

$$\nabla_{\bar{z}} \bar{\gamma}_n^*(\bar{z}) = \bar{P}^\top \bar{\Sigma}^{-1} \mathcal{H}_n(\bar{z}),$$

where $\mathcal{H}_n(\bar{z})$ denotes the inverse Hessian matrix $(\bar{\Sigma}^{-1} + \nabla^2 \text{Barr}(b_n \bar{\gamma}_n^*(\bar{z})))^{-1}$. Here, we note that the (diagonal) Hessian of the barrier function is positive definite for all \bar{z} , which implies $\|\mathcal{H}_n(\bar{z})\|_2 \leq \|\bar{\Sigma}\|_2$ uniformly over all n and $\bar{z} \in \mathcal{C}$. That is,

$$\nabla_{\bar{z}} (b_n)^{-2} \log J_\phi(b_n \bar{\gamma}_n^*(\bar{z}); \mathcal{U}) = (b_n)^{-1} \bar{P}^\top \bar{\Sigma}^{-1} \mathcal{H}_n(\bar{z}) \left(\nabla_x \log J_\phi(x; \mathcal{U}) \Big|_{b_n \bar{\gamma}_n^*(\bar{z})} \right).$$

To compute the Hessian, we will use the following identity

$$\frac{\partial A(x)b(x)}{\partial x} = \frac{\partial A(x)}{\partial x} \times_2 b(x)^\top + A(x) \frac{\partial b(x)}{\partial x}, \quad (43)$$

where $A(x)b(x)$ denotes a matrix-vector product; the 3-dimensional tensor $\frac{\partial A(x)}{\partial x}$ is summed across its second dimension in the first term of (43). Observe that the element-wise derivatives of \mathcal{H}_n with respect to the entries of $\bar{\gamma}_n^*(\bar{z})$ are given by

$$\frac{\partial}{\partial (\bar{\gamma}_n^*)_\ell} [\mathcal{H}_n(\bar{z})]_{ij} = -b_n \nabla_{\ell\ell\ell}^3 \text{Barr}(b_n \bar{\gamma}_n^*(\bar{z})) [\mathcal{H}_n(\bar{z})]_{i\ell} [\mathcal{H}_n(\bar{z})]_{\ell j}, \quad (44)$$

involving the third derivatives of the barrier function. Then, plugging into the first term of (43), we get

$$\begin{aligned} & -b_n \sum_j \nabla_{\ell\ell\ell}^3 \text{Barr}(b_n \bar{\gamma}_n^*(\bar{z})) [\mathcal{H}_n(\bar{z})]_{i\ell} [\mathcal{H}_n(\bar{z})]_{\ell j} [\nabla J_\phi(b_n \bar{\gamma}_n^*(\bar{z}); \mathcal{U})]_j \\ & = -b_n \nabla_{\ell\ell\ell}^3 \text{Barr}(b_n \bar{\gamma}_n^*(\bar{z})) [\mathcal{H}_n(\bar{z})]_{i\ell} \sum_j \left([\mathcal{H}_n(\bar{z})]_{\ell j} [\nabla J_\phi(b_n \bar{\gamma}_n^*(\bar{z}); \mathcal{U})]_j \right). \end{aligned}$$

Elementwise (row i and column ℓ), this matrix has the same entries as $\mathcal{H}_n(\bar{z})$, but with the ℓ th column scaled by

$$-b_n \nabla_{\ell\ell}^3 \text{Barr}(b_n \bar{\gamma}_n^*(\bar{z})) [\mathcal{H}_n(\bar{z}) \nabla J_\phi(b_n \bar{\gamma}_n^*(\bar{z}); \mathcal{U})]_\ell.$$

Let $b_n \mathcal{D}_n(\bar{z})$ be a diagonal matrix with these entries on its main diagonal. Then the matrix in the first term of (43) is given by $\mathcal{H}_n(\bar{z}) \mathcal{D}_n(\bar{z})$. The second term of (43) equals

$$b_n \mathcal{H}_n(\bar{z}) \left(\nabla_x^2 \log J_\phi(x; \mathcal{U}) \big|_{b_n \bar{\gamma}_n^*(\bar{z})} \right).$$

Thus, $\nabla_{\bar{z}}(b_n)^{-2} \log J_\phi(b_n \bar{\gamma}_n^*(\bar{z}); \mathcal{U})$ equals

$$\bar{P}^\top \bar{\Sigma}^{-1} \mathcal{H}_n(\bar{z}) \left(\mathcal{D}_n(\bar{z}) + \nabla_x^2 \log J_\phi(x; \mathcal{U}) \big|_{b_n \bar{\gamma}_n^*(\bar{z})} \right) \mathcal{H}_n(\bar{z}) \bar{\Sigma}^{-1} \bar{P}.$$

Noting $\bar{P}^\top \bar{\Sigma}^{-1} \mathcal{H}_n(\bar{z}) = O(1)$ uniformly over n and \bar{z} , bounding (C) in operator norm follows by uniformly bounding the largest diagonal element of $\mathcal{D}_n(\bar{z})$, and the operator norm of $\nabla_x^2 \log J_\phi(x; \mathcal{U}) \big|_{b_n \bar{\gamma}_n^*(\bar{z})}$.

Bounds for both terms follow from an application of Lemma 1, along with the use of the observation that the third derivatives of the barrier function are decreasing. To complete the proof, it therefore suffices to show uniformly over $\bar{z} \in \mathcal{C}$, and for sufficiently large n , all the entries of $\bar{\gamma}_n^*(\bar{z})$ are bounded below by a constant η . To this end, we define the limit of $\bar{\gamma}_n^*(\bar{z})$ as $n \rightarrow \infty$:

$$\bar{\gamma}_\infty^*(\bar{z}) = \operatorname{argmin}_{\gamma > 0} \left\{ \frac{1}{2} \gamma^\top \bar{\Sigma}^{-1} \gamma - \gamma^\top \bar{\Sigma}^{-1} \bar{P} \bar{z} \right\}. \quad (45)$$

The image of a compact set \mathcal{C} under the continuous map $\bar{\gamma}_\infty^*(\cdot)$ is compact and a subset of the positive orthant, which we call \mathcal{C}' . Define

$$\eta = \frac{1}{2} \min\{|x_j| : x \in \mathcal{C}'\} > 0.$$

Uniform convergence of $\bar{\gamma}_n^*(\bar{z})$ to $\bar{\gamma}_\infty^*(\bar{z})$ on a compact domain leads us to conclude

$$\min_j |[\bar{\gamma}_n^*(\bar{z})]_j| > \eta > 0,$$

for all $\bar{z} \in \mathcal{C}$ and sufficiently large n .

□

D Supplementary details: Section 6

We outline additional details involving the parameters in our numerical experiments below. For the simulation instances we generate in the atomic and balanced case analyses, each active coefficient has a random sign with magnitude $\sqrt{2t \log p}$. We let $t = 0.2$ for the low SNR setting, $t = 0.5$ for the moderate SNR setting, and $t = 1.5$ for the high SNR setting. In the heterogeneous scenario, the first predictor in the smallest active group has magnitude $\sqrt{2t \log p}/|T|$ and the last predictor in the largest group has magnitude $\sqrt{2t \log p}$ with magnitudes linearly interpolated for intermediate active coefficients; T is the number of signal variables in the instance. Each coefficient assumes a random sign and we set t for the low, medium, and high SNR as our previous cases.

For the selection step, we set the grouped penalty weights:

$$\lambda_g = \lambda \rho \sigma^2 \sqrt{2 \log p \frac{|g|}{\bar{g}}}$$

for solving the Group LASSO in both the randomized (PoSI) and non-randomized formulations (Naive and Split). Note, ρ is the proportion of data used for the query, $|g|$ is the number of features in group g , and \bar{g} is the floor of the average group size. This parameter assumes the value 1 for our methods and the Naive approach, and is set according to the training proportion for the two variants of Split. Clearly, in our balanced settings, we impose a uniform penalty across all groups, while the penalties for the heterogeneous settings scale with the size of our groups.

Addressing selection-informed inference post the Group LASSO, the barrier function used in our optimization problem (see Theorem 3.2) is given by

$$\text{Barr}(\gamma) = \sum_{g \in \mathcal{G}_E} \log(1 + (\gamma_g)^{-1}).$$

Observe, this choice of penalty assigns higher preference to optimizing variables away from the boundary of the selection region $[0, \infty)^{\mathbb{R}^{|\mathcal{G}_E|}}$. For executing the sampler, we set the

initial draw as follows

$$\beta^{(0)} = \widehat{\beta}_E,$$

the refitted least squares estimate in our setup. Completing our specifications, the inferential results we report in Section 6 are based upon 1500 draws of the Langevin sampler. We discard the first 100 samples as burn-in retaining the remainder for uncertainty estimation.